Journal of Environmental Management 397 (2026) 127486

Contents lists available at ScienceDirect

Journal of Environmental Management

journal homepage: www.elsevier.com/locate/jenvman

Research article

Characterization and modeling approach for planning restoration strategies in a complex basin affected by acid mine drainage

Jonatan Romero-Matos [a,*], Laura Sánchez-López [a], Rafael León [a], Robert L. Runkel [b], D. Kirk Nordstrom [c], Carlos R. Cánovas [a], Francisco Macías [a], José Miguel Nieto [a]

[a] Department of Earth Sciences & Research Center on Natural Resources, Health and the Environment. University of Huelva, Campus "El Carmen", 21071, Huelva, Spain
[b] U.S. Geological Survey, Colorado Water Science Center, Denver, CO, USA
[c] U.S. Geological Survey (formerly retired), USA

ARTICLE INFO

Keywords:
Metal-fluxes
Geochemical modeling
Iron precipitation
Water management
Odiel River basin

ABSTRACT

The management of acid mine drainage (AMD) impacted catchments, such as the Odiel River basin, in southwestern Spain, prioritizes reclamation to meet water resources needs. Assessing water composition across its watercourses is needed to identify major AMD contributors and potentially guide remediation efforts. An equilibrium-based mixing model was developed to simulate AMD pollutant load reductions and estimate the impact of selective restorations on water quality in the Odiel River, particularly at the planned Alcolea Reservoir near its outlet. Sampling under varying flow conditions (average vs. high flow) showed a reduction in acidity transport (from 54.0 to 42.5 ton/day), attributed to greater neutralization effects during high flows. Over 90 % of metal-fluxes originate alone from the Riotinto (73.6 %), Tharsis (14.5 %), and San Telmo (5.00 %) mining districts, among many other mines. While geochemical model estimates fit well with observed data ($R^2 = 0.99$), some deviations in non-conservative constituents (i.e. pH, Fe and Al) were observed ($R^2 = 0.73–0.99$), likely due to uncertainties in solubility constants and redox/Fe speciation. After evaluating model reliability, two reduction scenarios (50 % and 100 %) were applied to the three primary sources. Full removal of contamination could subtantially improve impounded reservoir water quality, with pH values of 4.93 and 7.64, and a net acidity between 8.75 and 4.63 mg/L eq. $CaCO_3$ in both average and high flows, respectively. Such differences may be related to flow regime effects on water quality. However, a 50 % reduction is insufficient to meet drinking or irrigation standards, highlighting the need for full and appropriate reclamation. The model offers a management tool for decision-making in the restoration of the Odiel River basin and could be transferable to similar AMD-affected basins worldwide.

1. Introduction

Acid mine drainage (AMD) is currently regarded as one of the most critical environmental threats affecting water bodies worldwide due to mining activities, worsening water quality and directly restricting the development of surrounding areas, both socially and economically (Cánovas et al., 2007; Nordstrom, 2011; Olías et al., 2011; Blowes et al., 2014; Foulds et al., 2014). The release of acidity and metals, their transport, and the longevity of AMD processes, represent a major source of pollution whose treatment and possible solution have been the subject of much research in recent years (Kimball et al., 2007; Ayora et al., 2013; Kefeni et al., 2017; Tu et al., 2022; Elghali et al., 2023). The management of water resources in AMD-affected catchments must recognize and improve water quality in the face of growing societal pressures, demanding more water availability and other societal benefits.

Hence, characterization of all metal and acidity sources and their respective impact on river catchment water quality is essential. Subsequently, the metal and acidity pathways should be identified, with particular attention to in-stream processes that cause chemical changes in downstream areas, along with quantifying the contaminant mass loading. Targeting these aspects could ultimately optimize decision-making for administrators and mining companies in AMD-impacted catchments and make remedial options more efficient, saving costs. Prior to the adoption of restoration measures, involving large economic investments, some authors have used geochemical modeling as a tool for predicting water quality under different approaches (Paulson and

* Corresponding author.
E-mail address: Jonatan.romero@dct.uhu.es (J. Romero-Matos).

https://doi.org/10.1016/j.jenvman.2025.127486
Received 15 July 2025; Received in revised form 22 September 2025; Accepted 27 September 2025
Available online 19 December 2025

Balistrieri, 1999; Balistrieri et al., 2007; Runkel et al., 2012; Mosley et al., 2015; Ball et al., 2004; Cravotta III, 2021; Rossi et al., 2021; Ryskie et al., 2024). However, most of these applications have been conducted at the scale of sites, reaches, or treatment systems (Runkel and Kimball, 2002; Nordstrom, 2020; Cravotta III, 2021). Geochemical modeling at the scale of large basins affected by AMD remains scarce and relatively underdeveloped in the literature (Li, 2019), which limits the information available for large-scale restoration planning.

The Odiel River basin is a prominent global example of a river network severely impacted by AMD, a consequence of mining activities dating back 5000 years, and is characterized by complex hydrological dynamics and a wide range of AMD sources (e.g., spoil heaps, adits, tailings, flooded open pits) (Cánovas et al., 2007; Nieto et al., 2013). The European Water Framework Directive, which aims to achieve a good chemical and ecological status of European waters (European Council, 2000), coupled with the future construction of the Alcolea Reservoir in the Odiel River (Olías et al., 2011; Cánovas et al., 2016), now halted but with a strong pressure exerted by politicians and irrigators to resume construction, make it necessary to take restoration measures within the basin, ensuring a water quality that complies with water policy (European Council, 2000) and meets guidelines for future uses (Ayers and Westcot, 1985; World Health Organization, 2022). However, the absence of gauging stations within the basin and the paucity of gauges installed in the numerous acid seeps limits the accurate calculation of the pollutant load transported by the basin's streams, restraining crucial information for its environmental management. In this context, the objectives of this work are: (1) to evaluate and quantify metal and acidity fluxes at a basin scale to prioritize remedial actions, and (2) to

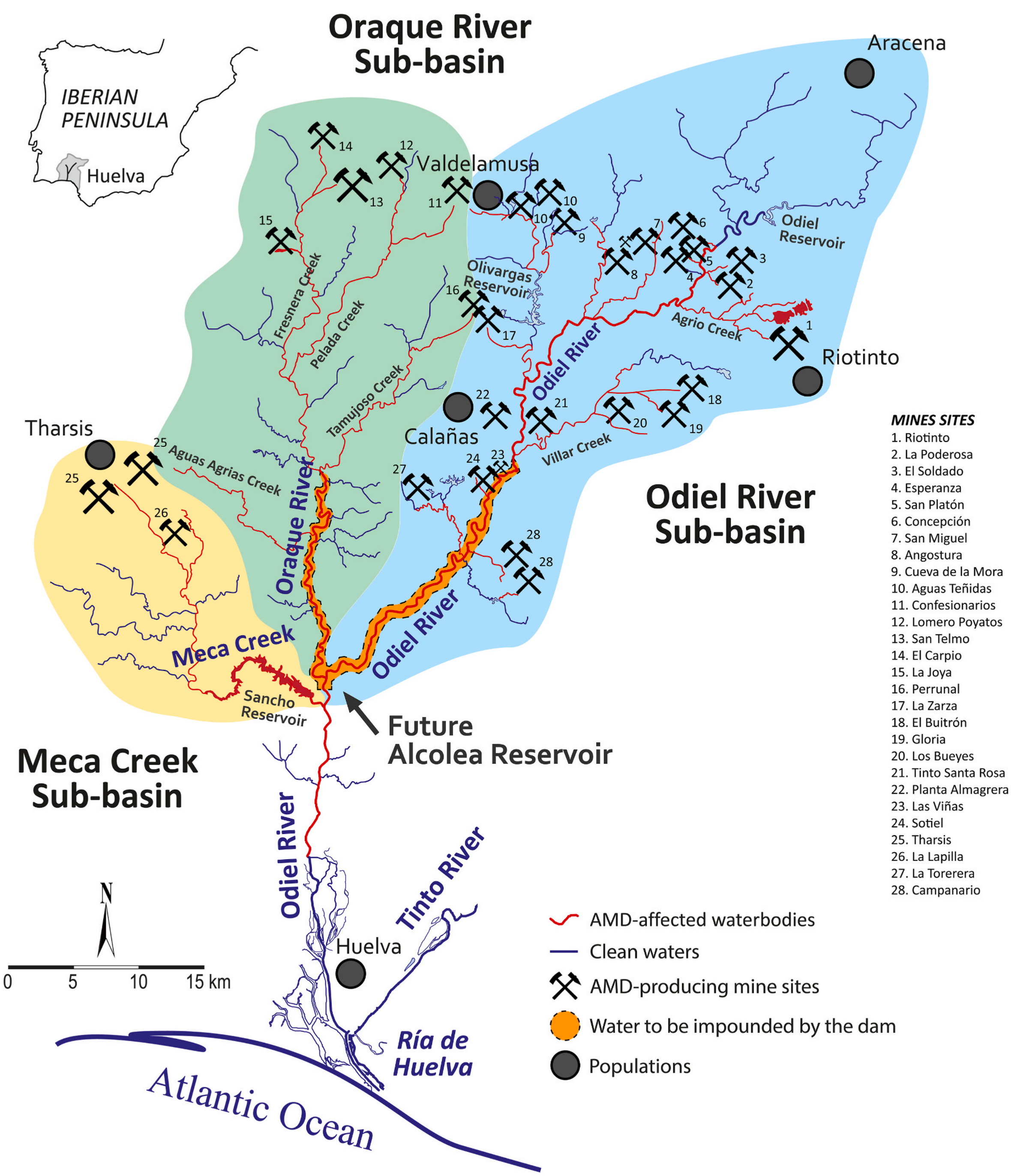

Fig. 1. Odiel River basin and the major effects of sulfide mining in its surface waters.

develop a geochemical equilibrium-based mixing model capable of predicting water quality under multiple remediation scenarios at the basin scale. Unlike previous applications of PHREEQC and similar tools, which have typically focused on single sites or river reaches, the proposed model integrates spatially distributed hydrological and geochemical data across a complex AMD basin, allowing assessment of basin-wide mixing and reactive processes and providing a practical tool to optimize economic resources for large-scale reclamation planning.

2. Materials and methods

2.1. Study area

The Odiel River basin, located in the southwest of the Iberian Peninsula (Fig. 1), is the largest drainage network in the province of Huelva, covering approximately 2300 km^2. The Odiel River flows mostly through materials of the Iberian Pyrite Belt (IPB), where it meets its main tributaries, Oraque and Meca rivers (Fig. 1). Annual average precipitation ranges from 600 mm in the lower drainage basin to 1000 mm in the upper part, with almost 50 % occurring between November and January, while summer precipitation is practically non-existent. However, strong seasonal and interannual variations exist as response of the Mediterranean climate, with prolonged drought periods and intense but short rain episodes (Olías et al., 2006; Cánovas et al., 2007). The Odiel River flows together with the Tinto River into the Ría de Huelva estuary, discharging huge metal and acidity loads into the Atlantic Ocean (Pérez-López et al., 2023), along with other contributions of industrial and urban origin (e.g., phosphogypsum stack; Davis et al., 2000; Millán-Becerro et al., 2023).

The intense mining activity developed in the IPB, especially from the mid-19th century until the late 20th century, has resulted in the degradation of most waterbodies in the region due to the generation of AMD (Nieto et al., 2013) (Fig. 1). In fact, the cessation of mining activities caused a further degradation of the water quality due to interruption of environmental controls. Currently, some legacy mines (Riotinto, Aguas Teñidas and Sotiel mines) have reopened, assuming past environmental liabilities and performing exhaustive environmental controls, with documented improvements in water quality (León et al., 2023). The reduction in AMD generation from legacy mine sites by mining companies, together with the implementation of future environmental restoration plans by public administrations (e.g., Macías et al., 2017a; Macías et al., 2017b; Cánovas et al., 2019; Orden et al., 2021; Remesal, 2024), would enhance the reclamation of the Odiel basin.

2.2. Water sampling and analysis

Flow regime strongly controls hydrochemistry and pollution levels in AMD-affected basins (Olías et al., 2006; Cánovas et al., 2007; Sarmiento et al., 2009). Two extensive sampling campaigns were performed in the Odiel River basin in January 2022 (10th to 13th) and February 2023 (February 13th to 16th) under different hydrological conditions. This design aimed to account for hydrological representativeness and to assess the potential influence of flow variability on water quality. Water samples were taken from the main watercourses, clean tributaries, AMD discharges and major confluences (n = 53 for each campaign), within the three main sub-basins of the Odiel River (Fig. 1). At confluences, samples were taken 100–150 m downstream to ensure effective mixing processes. All data is available in Supplementary Material (Tables S1 and S2).

Physicochemical parameters (i.e., pH, electrical conductivity (EC), redox potential (ORP), temperature) were measured in the field using a previously calibrated multiparameter probe (Hanna Instruments HI 9025 and HI 9033) and flow gauging was carried out with a flow meter (Global Water FP111). When feasible, flow measurements were conducted in at least one of the confluent tributaries. For those samples with a pH above or around 4.5, alkalinity was also determined by titration (CHEMetrics Total Titrets). Calibration of multimeters was conducted daily prior to fieldwork and verified throughout the day using standard solutions for pH (4.01, 7.00 and 10.01 at 25 °C using HORIBA Laqua solutions), and EC (84 μS/cm, 1413 μS/cm and 12.88 mS/cm at 25 °C using HORIBA Laqua solutions) whereas ORP was checked using 220 mV and 468 mV solutions from HACH SensION + at 25 °C. Redox potential measurements were corrected to the standard hydrogen electrode (Nordstrom and Wilde, 1998). Water samples were stored in polyethylene bottles after filtration with cellulose nitrate filters (0.45 μm), acidified to pH < 2 with HNO_3 suprapure and subsequent refrigeration until chemical analysis.

Field determination of Fe(II)/Fe(III) was conducted during the February 2023 campaign by colorimetry, following complexation with the addition of a 0.5 % (w/w) 1.10-phenanthrolinium chloride solution to each filtered sample (Tamura et al., 1974). The analyses were conducted using a DR/890 portable colorimeter (HACH), with a detection limit of 0.3 mg/L and a precision >5 %.

Samples, other than Fe(II)/Fe(III) determinations, were analyzed at the Central Research Services of the University of Huelva by Inductively Coupled Plasma-Optical Emission Spectroscopy (ICP-OES; Jobin Yvon Ultima 2) for major elements and by Inductively Coupled Plasma-Mass Spectrometer (ICP-MS; Agilent 7700) for trace elements, although in this work only the most relevant elements are included (i.e. Fe, Al, S, Mg, Na, Mn, Cu and Zn). To assess the analytical precision, triplicate analyses were performed, yielding results below 5 % (%RSD) for all constituents. In each analysis sequence, control blanks were added, with element concentrations below the detection limits in each blank. The analytical accuracy was confirmed by the analysis of reference materials (NIST-1640). Dissolved sulfate concentrations were calculated from dissolved sulfur (S) concentrations, assuming minor presence of other species (Reisman et al., 2007). This assumption was confirmed using the geochemical code PHREEQC (Parkhurst and Appelo, 2013), and sulfate determination by ion chromatography (IC), to check QA/QC of the analytical data regarding this constituent that usually produces the largest source of error in the charge balance. Charge balance calculated by PHREEQC (Parkhurst and Appelo, 2013) showed errors below 15 %, with most samples in the range of ±5 %.

The Net Acidity (NA) was estimated using the original formula proposed by Kirby and Cravotta III (2005), which includes both proton acidity relative to pH and metal acidity related to the hydrolyzable metals (Fe, Al and Mn), modified to consider other important hydrolyzable elements such as Zn and Cu (Eq. (1)):

$$\mathbf{NA\ [mg/L\ eq.\ CaCO_3]} = \mathbf{50045} \cdot \mathbf{(3C_{Al} + 2C_{Fe} + 2C_{Mn} + 2C_{Zn} + 2C_{Cu} + 10^{-pH}) - Alk} \qquad \text{Eq. 1}$$

where $\mathbf{C_x}$ is the molar concentration of Al, Fe, Mn, Zn and Cu (mmol/L) and **Alk** is the total alkalinity (mg/L equivalents of $CaCO_3$). This estimation is semi-quantitative because of the inherent problems with defining acidity (Kirby and Cravotta, 2005b)

2.3. Mixing ratios and constituent loads

The simultaneous application of multiple conservative tracers in the calculation of mixing ratios through solute mass balance (Eq. (2)) is a convenient approach for AMD waters (Schemel et al., 2006; Runkel et al., 2013; Pelizardi et al., 2017; Cánovas et al., 2017), resulting in a series of mean end-member ratios for the various mixtures under consideration (i.e. confluences):

$$\mathbf{C_M} = \sum \mathbf{C_{EM}} \cdot \boldsymbol{(Q_i/Q_T)} \qquad \text{Eq. 2}$$

where $\mathbf{C_M}$ is the concentration of a conservative constituent within a mixture (i.e. below the confluence); $\mathbf{C_{EM}}$ is the concentration of the same constituent in the end-members (i.e. tributaries and main watercourse above the confluence); and $\boldsymbol{Q_i/Q_T}$ where Q_i is the streamflow associated with the end-member and Q_T is the total flow from all the end members, which refers to the volumetric and chemical proportion of each tributary, discharge or main watercourse within the several confluences of the basin; i.e. the mixing ratio of each end-member contributing to the mixture. C_M is the observed concentration and $C_{M'}$ is the estimated concentration of the mixture calculated using Eq. (2).

Calculated mixing ratios were then used to estimate streamflow where technical feasibilities did not allow to directly measure flow on the main stem. In this case, Eq. (2) is rearranged to account for Q_T or Q_i where streamflow is missing. Calculation can be consulted on Tables S3 and S4.

The selection of these tracers requires a comprehensive understanding of the system, in this case, the Odiel River basin. After examination of all potential conservatives analytes; sulfate, Mg and Na have been selected as end-member constituents since they commonly show a conservative behavior during both synoptic samplings carried out and other studies (Olıas et al., 2004; Cánovas et al., 2007; Cánovas et al., 2012), and their concentrations vary significantly between sources.

The dissolved metal load (DML of Al, Fe, Mn, Cu and Zn, in kg/day), net acidity load (NAL in kg/day eq. of $CaCO_3$) and sulfate load (SOL in kg/day) were calculated for each sampling point by simply multiplying the concentration of dissolved constituent concentrations by the streamflow.

2.4. Conceptual model

The basin-scale geochemical model was developed using the PHREEQC v3.7 code (Parkhurst and Appelo, 2013) and the *wateq4f.dat* thermodynamic database (Ball and Nordstrom, 1991), extended with the thermodynamic data of the main mineral phases controlling the geochemical processes in the AMD waters of the Odiel basin (Sánchez-España et al., 2011; Caraballo et al., 2013). The conceptual framework is based on downstream modeled mixtures as analogs to the actual water confluences within the basin. The “MIX” command serves as the basis of the mixing model, which enables mixing of two or more aqueous solutions at different ratios, previously calculated by mass balance approach. Given that significant geochemical processes occur during the mixing in river confluences, the “EQUILIBRIUM_PHASES” command was included to incorporate equilibrium reactions involving Fe and Al mineral phases. Well-aerated conditions were maintained through constant atmospheric partial pressure of O_2 ($\log P(O_2) = -0.7$) and CO_2 ($\log P(CO_2) = -3.5$) equilibrium. Most of the geochemical processes in AMD of the IPB are controlled by precipitation of schwertmannite ($Fe_8O_8(OH)_{8-2x}(SO_4)_x \bullet nH_2O$, where $1 < x < 1.75$) and basaluminite ($Al_4(SO_4)(OH)_{10} \bullet 5H_2O$), which typically precipitates at pH 2.0–4.0 and 4.5–5.0 respectively. Basaluminite could be considered as a nanomineral variety of felsőbányite, however, the former will be used as it is commonly found in acidic sulfate waters and has been widely documented in the geochemical literature. Attenuation of Fe and Al in surface water by schwertmannite and basaluminite precipitation has been reported in previous works (Bigham and Nordstrom, 2000; Sánchez-España et al., 2011; Caraballo et al., 2013; Lozano et al., 2018; Schoepfer and Burton, 2021) and in this study, as evidences the FESEM-EDS images of solids retained in the filters during sampling (Fig. S1). For this model, minor geochemical processes (i.e. surface complexation, sorption, coprecipitation) involved in reactive transport processes under low pH conditions (i.e. this work) were not incorporated.

Once mixing is modeled in the upper part of the basin, the final solution is again allowed to mix with the next watercourse downstream from this mixing point, until reaching the Alcolea Reservoir flooding area, the outlet of the model. A schematic modeling diagram of the whole basin is illustrated in Fig. S2. Modeled values will then be compared to observed values in confluences to assess the reliability of the model. Once the model has been optimized for conservative tracers and non-conservative constituents are behaving as predicted for dilution, buffering, Fe oxidation, and Fe and Al precipitation, then a baseline condition will have been established against which remediation scenarios can be considered.

3. Results and discussion

3.1. Hydrological context

The Mediterranean climate of the study area is characterized by significant seasonal variability in terms of annual precipitation, with typical rainy seasons from October to March, marked by sporadic but intense rainfall events (lasting a few hours or days). Annual precipitation patterns also exhibit considerable interannual variation, with periods of intense drought interspersed with higher precipitation regime years. Drought time series commonly last for 2 or 3 years, however, the current drought has been prolonged since 2015 according to Standardized Precipitation Evapotranspiration Index (SPEI) values below 0, and more intensely from 2018 to 2023 (SPEI <1) (Vicente-Serrano et al., 2017). The two sampling campaigns were carried out during 2022 and 2023, so the hydrochemical conditions recorded correspond to the 2018-2023 drought period (Fig. 2).

Streamflow data is very limited due to the lack of gauging stations in the basin, hindering the evaluation of streamflow data temporal series. Currently, only one gauging station at Sotiel Coronada, situated about 20 km upstream of the Alcolea dam, is part of the Automatic Hydrological Information System of the Andalusian regional government (Dirección General de Infraestructuras del Agua, 2024). Sampling campaigns were conducted following precipitation events, yielding mean values of 323 L/s in January 2022 and 1313 L/s in February 2023 (Fig. 2) at Sotiel. Both samplings events were undertaken during a period of medium and high waters levels, respectively, as their flows exceed the 50th (70 L/s) and 75th (590 L/s) percentiles calculated for the period 2021-24, previously regarded as a drought period. Measured and estimated flows are found in Tables S5 and S6, along with uncertainties (RSME; r^2) associated with flow estimations.

3.2. Hydrogeochemistry and pollutant loads evaluation

A description of the evolution of acidity and selected metal loads recorded in this work is provided in this section. The entire dataset can be found in Supplementary Material (Tables S1 and S5 for January 2022 and Tables S2 and S6 for February 2023). Figs. 3 and 4 show the variation of pH, NA and dissolved metal loads through the Odiel and Oraque sub-basins during the sampling of January 2022 (i.e. average-flow). In both sampling periods, the river exhibits good water quality and riparian vegetation from its headwaters until the confluence of the first acidic leachates (Fig. 3), which result in a slight increase in acid load and a decline in pH values (OD1). An irreversible change takes place after the confluence of the Agrio Creek, which collects acidic leachates from the Riotinto Mines, and dramatically increases the acid load of the Odiel River, reducing the pH to values below 3 in both periods (OD2) (Fig. 3 and S3). The Agrio Creek corresponds to one of the most important tributaries on the left bank (looking downstream) of the basin, with extreme concentrations of pollutants (6.31–5.42 g/L eq. $CaCO_3$ of net acidity), being the main contributor of acidity due to its high flow volume compared to other acidic discharges (around 6 times more on average) (Tables S1, S2, S5 and S6) (Sarmiento et al., 2009; Galván et al., 2016; Cánovas et al., 2018a).

In January 2022, the net acidity (NAL), sulfate (SOL) and dissolved metals load (DML) increased up to 44.3, 76.0 and 11.0 ton/day of instantaneous load at OD2 (Fig. 3AB), respectively. This drastic increase leads to an unalterable deterioration of the Odiel River’s conditions until its discharge into the Huelva estuary, which is evident downstream, where the metallic load and pH (3.10) have not substantially improved prior to the confluence with the Oraque River (OD8) (Fig. 3A). The contributions of minor discharges, including La Zarza (ZR), Sotiel (SOT),

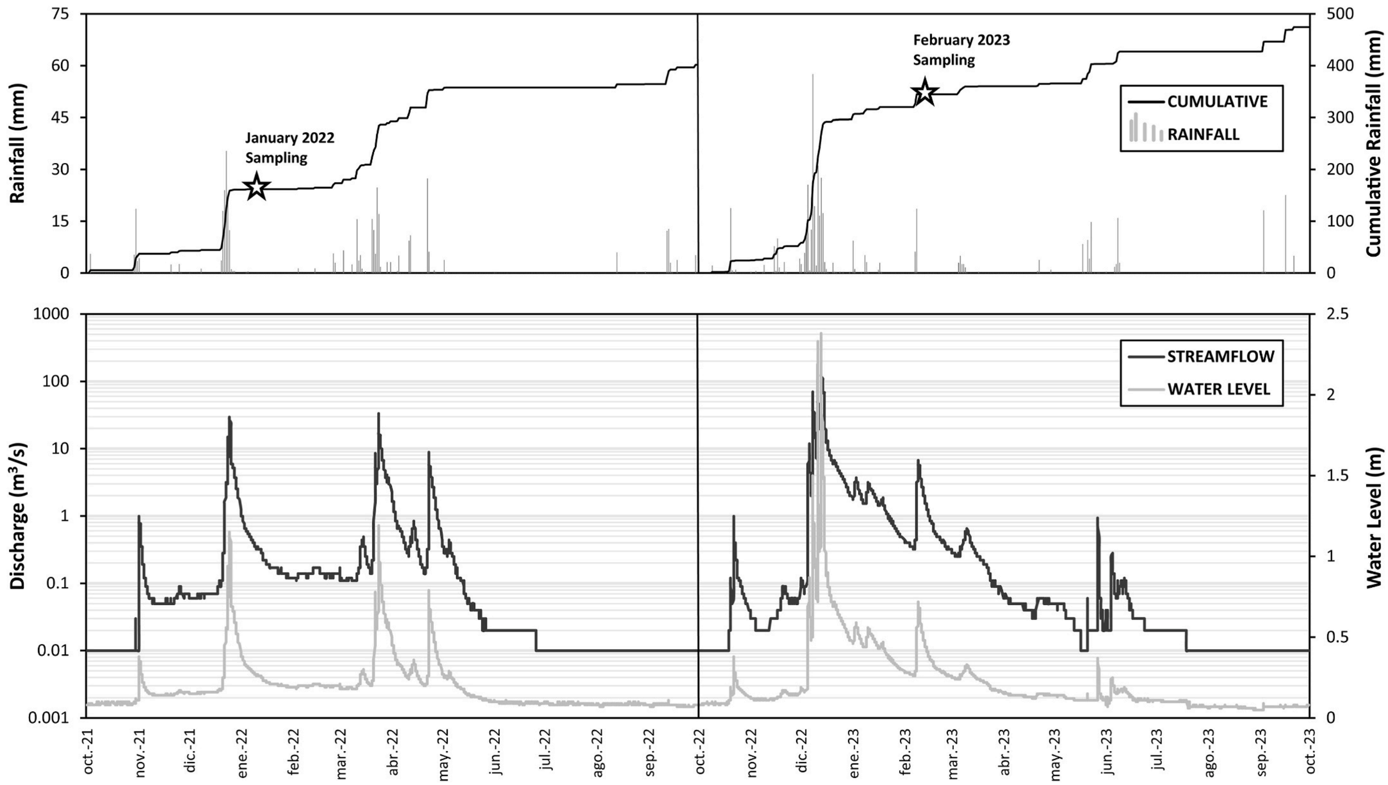

Fig. 2. Rainfall and discharge distribution and magnitude along the sampling periods at the Sotiel Coronada pluviometric-gauge station (January 2022 and February 2023). Center-oriented vertical line represents division between hydrological years.

Las Viñas (VÑ) or Almagrera (BAT) are relatively low (min.: 41.5 kg/day; max.: 568 kg/day of DML) in comparison to the AG input. Acidic conditions are persistent despite the presence of alkaline or slightly affected streams with flows of the order of tens of L/s (e.g., Escalada Creek, Olivargas Creek and Villar Creek) (Fig. 3A). The main tributary of the Odiel is the Oraque River (Fig. 1), which is polluted by the leachates of San Telmo Mine (ST1 and ST2), Tharsis (RAA) and other minor acid discharges (Fig. 4). The confluence of acidic leachates from San Telmo has resulted in a NAL, SOL and DML of 3.61, 6.97 and 1.00 ton/day, respectively, in the Oraque headwaters (FRE2). The Oraque River undergoes considerable neutralization and dilution processes along its main course due to the inflow of clean water streams (Tamujoso Creek and others), despite the acidic input from the Pelada Creek (PEL4) (Fig. 4). Prior to its confluence with the Odiel River (OR3), the Aguas Agrias Creek (RAA), originating from the Tharsis Mines (Fig. 4A), markedly elevates the Oraque's load up to 6.08 ton/day of NAL, 14.1 ton/day of SOL and 1.43 ton/day of DML (Fig. 4). The Oraque's load increase has a detrimental impact on the lower Odiel River basin, increasing the transported load from 47.0, 87.5 and 10.4 ton/day to 54.0, 105 and 11.6 ton/day of NAL, SOL and DML, respectively, following the confluence, where the Alcolea Reservoir will be located (OD9) (Fig. 3).

Figs. S3 and S4 display the variation of pH, NA and dissolved metal loads through the Odiel and Oraque sub-basins during the sampling of February 2023 (i.e. high flow). As can be seen, the NAL, SOL and DML increased up to 116, 206 and 29.4 ton/day, respectively at OD2 (Fig. S3), due to the higher flow values recorded (Fig. 2) compared to the previous sampling. However, there is a clear improvement in downstream conditions before the confluence with the Oraque River (OD8), with 31.8 ton/day of NAL, 81.5 ton/day of SOL and 7.46 ton/day of DML, and a pH value of 4.05 (Fig. S3). These comparatively smaller loads could be due to the higher clean water inflows during this period that could enhance neutralization of acidity and metals transported by the main watercourse. Whereby acidic waters mix with clean waters inflows, precipitation of Fe and Al mineral phases (mainly oxy-hydroxysulfates as schwertmannite and basaluminite) occur along with other metals through sorption and co-precipitation processes (Bigham and Nordstrom, 2000; Sánchez-España et al., 2011; Macías et al., 2012; Carrero et al., 2015; Papaslioti et al., 2024). NAL and DML are somewhat lower than in January 2022 at OD8 (Fig. 3B), however, SOL is higher in this period probably due to the more conservative behavior of sulfate and the higher flows. On the other hand, the Oraque River shows higher increments in load in its headwaters (FRE2) compared to average-flow conditions (Fig. 4), with 5.38 ton/day of NAL, 10.5 ton/day of SOL and 1.57 ton/day of DML (Fig. S4). A neutralization effect is also recorded along the main rivercourse, evidenced by a decrease in the NAL (2.48 ton/day) and DML (0.63 ton/day) (Fig. S4), although their values are still higher than in January 2022 (OR2) (Fig. 4). Sulfate still behaves conservatively and the SOL (13.1 ton/day) prior to Aguas Agrias Creek has a higher value than in the San Telmo Mine area (FRE2) (Fig. S4B). Aguas Agrias Creek (RAA) causes an increase in NAL, SOL and DML at OR3 with respective values of 10.8, 30.1 and 2.60 ton/day (Fig. S4). Oraque River discharges into the Odiel River causing an increase in loads of up to 42.5 ton/day of NAL, 111 ton/day of SOL and 9.83 ton/day of DML at the Alcolea Reservoir site (OD9) (Fig. S3).

Highest mass loadings are mainly attributed to AG, which accounts for 64.4 % of NAL and 68.0 % of SOL contributions during the average-flow campaign, considering all inflows, followed by RAA with 18.7 % of NAL and 20.8 % of SOL and by ST with 5.93 % of NAL and 5.54 % of SOL. The same trend was observed during high-flow conditions, however, AG significantly increased its contribution up to 77.1 % of NAL and 84.7 % of SOL. Both RAA and ST contributions decreased (9.00 % of NAL and 11.4 % of SOL; 4.14 % of NAL and 4.38 % of SOL; respectively) compared to average flows but they are still the two main inputs following AG. Most sources increased their mass loadings during February 2023 relative to January 2022 (Tables S5 and S6). A comparison between the sum of loads from all sources with the estimated load at the Alcolea Reservoir point (OD9) allows for the determination

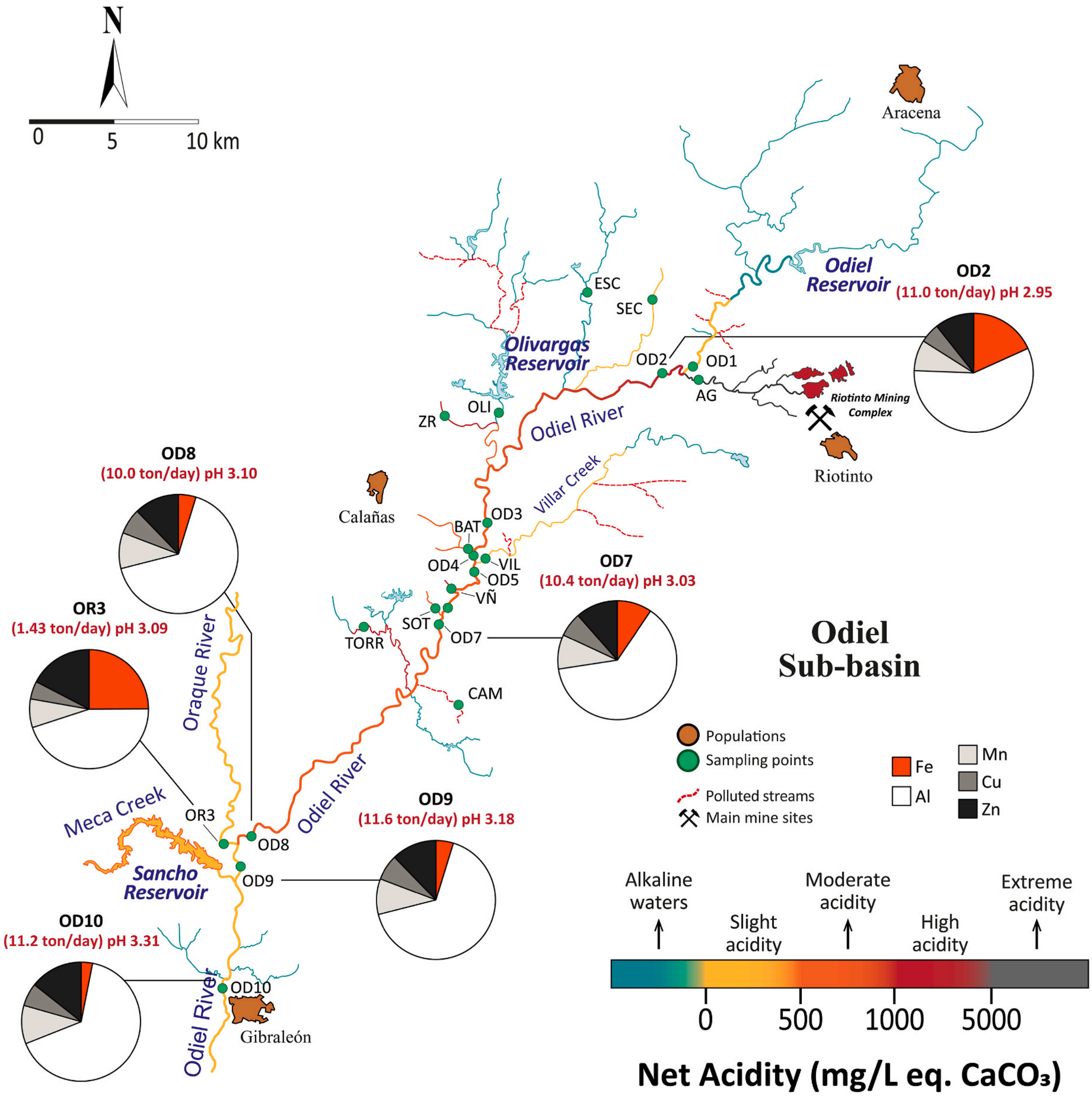

Fig. 3. A. Contamination map based on net acidity in the reaches of the Odiel River sub-basin during the January 2022 sampling (average-flow). Ranges of net acidity are illustrated using a 5-color scale (extreme acidity, >5000 mg/L; high acidity, 1000–5000 mg/L; moderate acidity, 500–1000 mg/L; slight acidity, 0–500 mg/L; and alkaline waters). Dissolved metal loads (Fe, Al, Mn, Cu and Zn) and pH are also shown, along with pie charts representing metal proportion, in the main watercourse. B. Evolution of the net acidity and sulfate loads in the main watercourse and its multiple inflows (AMD sources, clean waters and main tributaries). Note that inflow loading scales are logarithmic.

of the percent retention for different metals within the basin. For January 2022, 19.0 % of NAL, 8.73 % of SOL and 39.1 % of DML were retained within the basin, before reaching Alcolea Reservoir. These retention processes were related to Fe precipitation as previously reported by Sánchez-España et al. (2005), given that 91.1 % of the total Fe contributed by sources did not reach the referenced site (OD9). In February 2023, higher flows led to more intense neutralization processes, with more pronounced retention than January 2022 (68.9 % of NAL, 56.6 % of SOL and 76.4 % of DML were retained), generally consistent with winter-spring high-flow periods (Cánovas et al., 2018a). For that period, Fe is the most affected metal (95.0 %), but with Al, Mn, Cu and Zn retention levels above 50 %. The study of mass loadings originating from tributaries have allowed us to conclude that the main metal-fluxes in the Odiel basin come from the Riotinto Mining Complex, the Tharsis Mines and the San Telmo Mine, as previously reported (Sarmiento et al., 2009; Cánovas et al., 2012; Galván et al., 2016), justifying the prioritization of remediation measures in these three mine sites due to their potential significant impact on the Alcolea Reservoir water quality. Further monitoring should be conducted across other low-flow seasons such as summer and autumn, when contrasting patterns to these findings (i.e., higher concentrations and washout processes) have been observed (e.g. Cánovas et al., 2018a), supporting robust long-term management strategies.

3.3. Basin-scale geochemical model

3.3.1. Model reliability

An equilibrium-based geochemical model was performed at the basin scale. Supplementary Material presents the entire data incorporated into the model and respective outputs (i.e. calculated mixing ratios in Tables S3 and S4; observed and estimated concentrations through PHREEQC mixing model in Table S7). Model reliability is important for

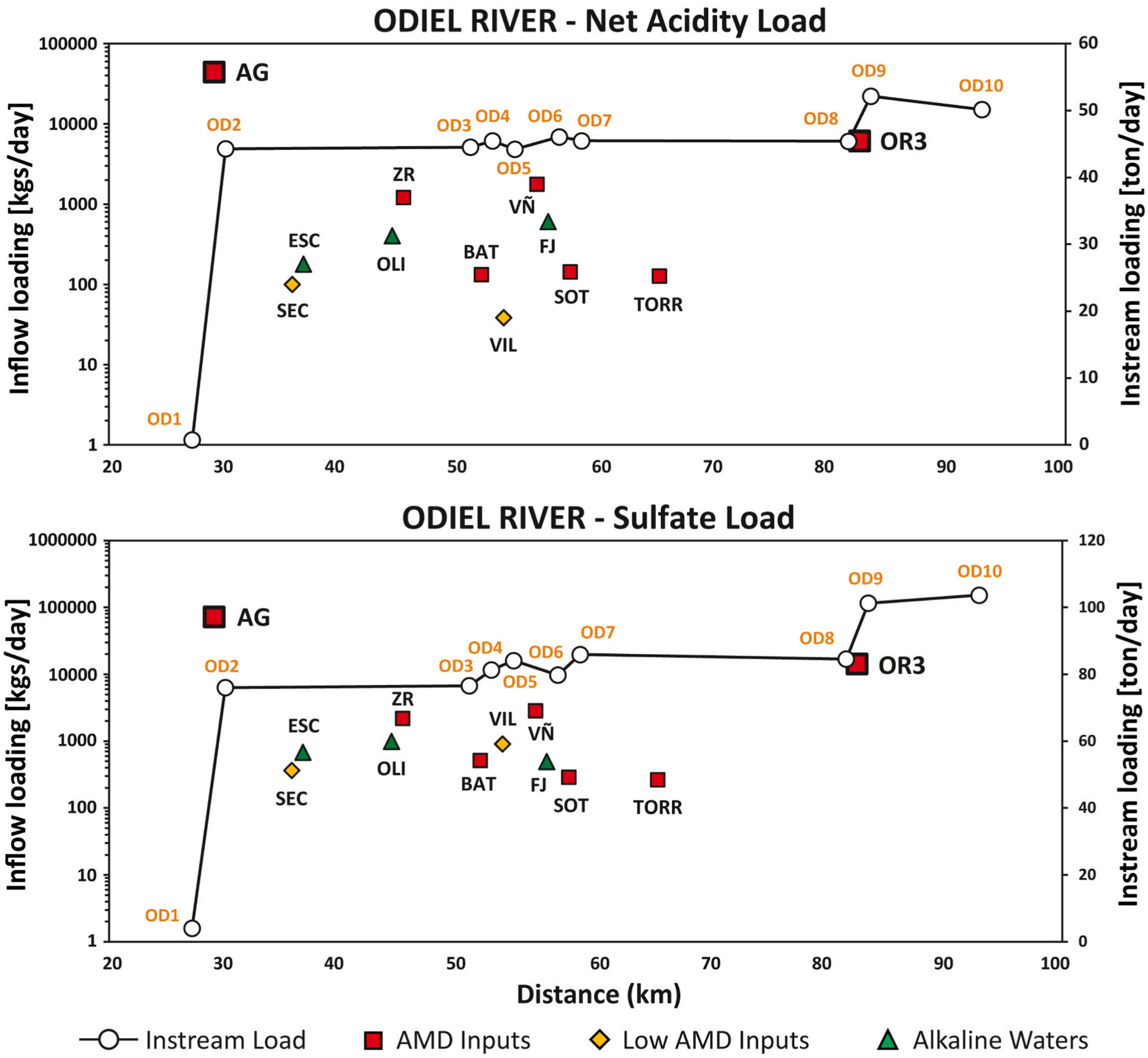

Fig. 3. (*continued*).

predicting hydrochemical conditions at the basin scale, ultimately conceptualizing metal and acidity sources, their interactions and fate (Nordstrom, 2012). The appropriateness of this model is assessed by comparing observed and estimated concentrations of conservative elements (Balistrieri et al., 2007; Mosley et al., 2015; Rossi et al., 2021; Ryskie et al., 2024), other than those used for calculating mixing ratios (i.e., sulfate, Mg and Na). Associated uncertainties should be labelled for strict evaluation of a model (Nordstrom and Campbell, 2014). Non-conservative elements such as pH, Fe and Al are strongly influenced by geochemical processes (i.e., hydrolysis and precipitation processes).

Fig. 5 shows a conservative behavior for most of the estimated constituents. As anticipated, Fe is typically overestimated in the model since it is undergoing precipitation during mixing processes (Sarmiento et al., 2009; Ryskie et al., 2024). These precipitation processes have a great impact on the prediction of pH values, with lower values generally observed in the river compared to the estimates (Fig. 5 and Table S7A and S7C). Iron hydrolysis reactions, such as schwertmannite precipitation, releases protons, decreasing the pH or buffering it when an inflow of higher pH mixes with the main river (Bigham and Nordstrom, 2000). Aluminum is notably well estimated due to its conservative behavior at pH < 4.5 (Nordstrom and Ball, 1986; Bigham and Nordstrom, 2000) (Fig. 5 and Table S7). During both sampling campaigns, only the Tamujoso Creek and the mid to lower part of the Oraque sub-basin achieved pH values greater than 4.5 (Table S7), limiting Al precipitation elsewhere. In fact, most waters were undersaturated in basaluminite and oversaturated in schwertmannite, according to PHREEQC calculations (Tables S1 and S2 show saturation indexes for the observed dataset; Table S7 shows saturation indexes for the conservative approach modeled data). In contrast, slight overestimations for some modeled element concentrations may be related to sorption/co-precipitation processes occurring in mixing sites, which is not considered in our model, particularly during higher flows of February (Fig. 5), as higher pH values should result in greater mineral precipitation and consequent sorption (Webster et al., 1998; Paulson and Balistrieri, 1999; Nordstrom, 2011; Carrero et al., 2015) (see also Fig. S1B for possible Cu presence on basaluminite). Therefore, in a real remediation scenario where stream pH is expected to increase, elements that currently behave conservatively under acidic conditions (e.g., Mn, Cu, Zn) would likely become more reactive. It may be inferred that remedial simulations will likely underestimate removal and, consequently, the anticipated improvement in water quality, as predicted by the model, will be of smaller magnitude than actual remediation results (Runkel et al., 2012).

3.3.2. *Modified geochemical equilibrium model with Fe and Al minerals*

Considering the deviations observed between measured and modeled values for pH, Fe and to a lesser extent Al, schwertmannite and basaluminite equilibrium reactions were applied to the mixing model, with solubility product constants from Bigham et al. (1996)

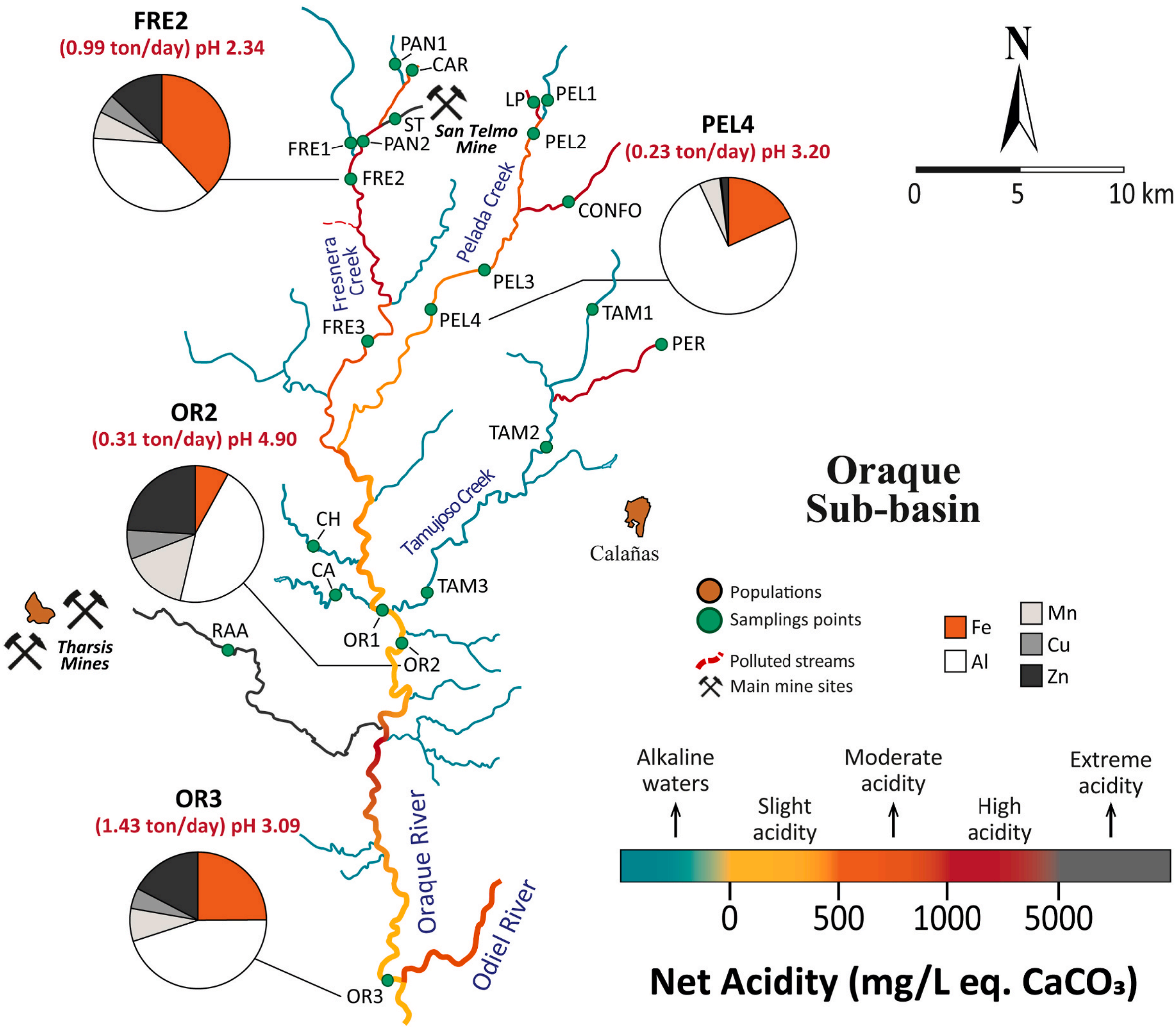

Fig. 4. A. Contamination map based on net acidity in the reaches of the Oraque River sub-basin during the January 2022 sampling (average-flow). Ranges of net acidity are illustrated using a 5-color scale (extreme acidity, >5000 mg/L; high acidity, 1000–5000 mg/L; moderate acidity, 500–1000 mg/L; slight acidity, 0–500 mg/L; and alkaline waters). Dissolved metal loads (Fe, Al, Mn, Cu and Zn) and pH are also shown, along with pie charts representing metal proportion, in the main watercourse. B. Evolution of the net acidity and sulfate loads in the main watercourse and its multiple inflows (AMD sources, clean waters and main tributaries). Note that inflow loading scales are logarithmic.

(schwertmannite; $\log K_{sp} = 18 \pm 2.5$) and Sánchez-España et al. (2011) (basaluminite; $\log K_{sp} = 23.9 \pm 0.7$), along with atmospheric equilibrium. The latter will allow ferrous iron to oxidize in mixing sites forming ferric iron and increasing its ion activity, for which schwertmannite saturation is strongly dependent on. Gypsum is also incorporated to test its possible influence on sulfate concentrations. The imposed equilibrium makes minerals precipitate only in case of oversaturation (for gases, a reservoir is included to attain equilibrium). Equilibrium-based mixing model results are shown in Fig. 6 and Table S7B. Aluminum and sulfate show negligible influence from equilibrium reactions, as basaluminite is predominantly undersaturated (SI < 0) and gypsum is nearly at equilibrium (SI ≈ 0) in most samples (Table S7). Sulfate removal by schwertmannite precipitation (Nordstrom, 2011) may be also considered volumetrically negligible (<5 %) given the high concentrations observed in waters throughout the basin. Jarosite incorporation in the model also seems to have little to no influence on estimations (Nordstrom, 2020; Ryskie et al., 2024), as all samples fall in the schwertmannite stability field (Caraballo et al., 2013). Iron and pH estimations have significatively improved, but with persistent deviations between modeled and measured values that can derived from several causes: 1) $\log K_{sp}$ influence on schwertmannite equilibrium modeling; 2) Iron oxidation kinetics; 3) Overestimation of schwertmannite saturation owed to iron colloids passing through filters (Nordstrom, 2011).

Variable stoichiometry and thermodynamic instability of schwertmannite calls for the consideration of its solubility as a "window" (Runkel et al., 1996; Bigham et al., 1996; Sánchez-España et al., 2011; Caraballo et al., 2013; Schoepfer and Burton, 2021) instead of a single value, that is, the solubility of this Fe phase should be modeled through a range of $\log K_{sp}$. Caraballo et al., (2013) proposed an apparent $\log K_{sp}$ range from 5.8 to 39.5, which can be statistically attributed to the specific characteristics of the water and schwermannite sample. Additionally, this range can also be statistically explained by pH alone (i.e. $\log K_{sp} = 11.2\,\mathrm{pH} - 15.6$; r2 = 0.74), as demonstrated by Caraballo et al., (2013) and Schoepfer and Burton (2021), thus simplifying solubility estimations. In this regard, two new approaches have been tested in the mixing model of January 2022: 1) Using $\log K_{sp} = 10.5 \pm 2.5$ from Yu et al. (1999) (Fig. S6A and Table S8A); 2) Setting variable $\log K_{sp}$ for each mixture in the aforementioned range (Fig. S6B and Table S8B).

Decreasing the solubility constant (from Bigham et al. (1996) to Yu et al. (1999)) results in an overall overestimation of the Fe precipitation, showing estimated values generally lower than observed (average

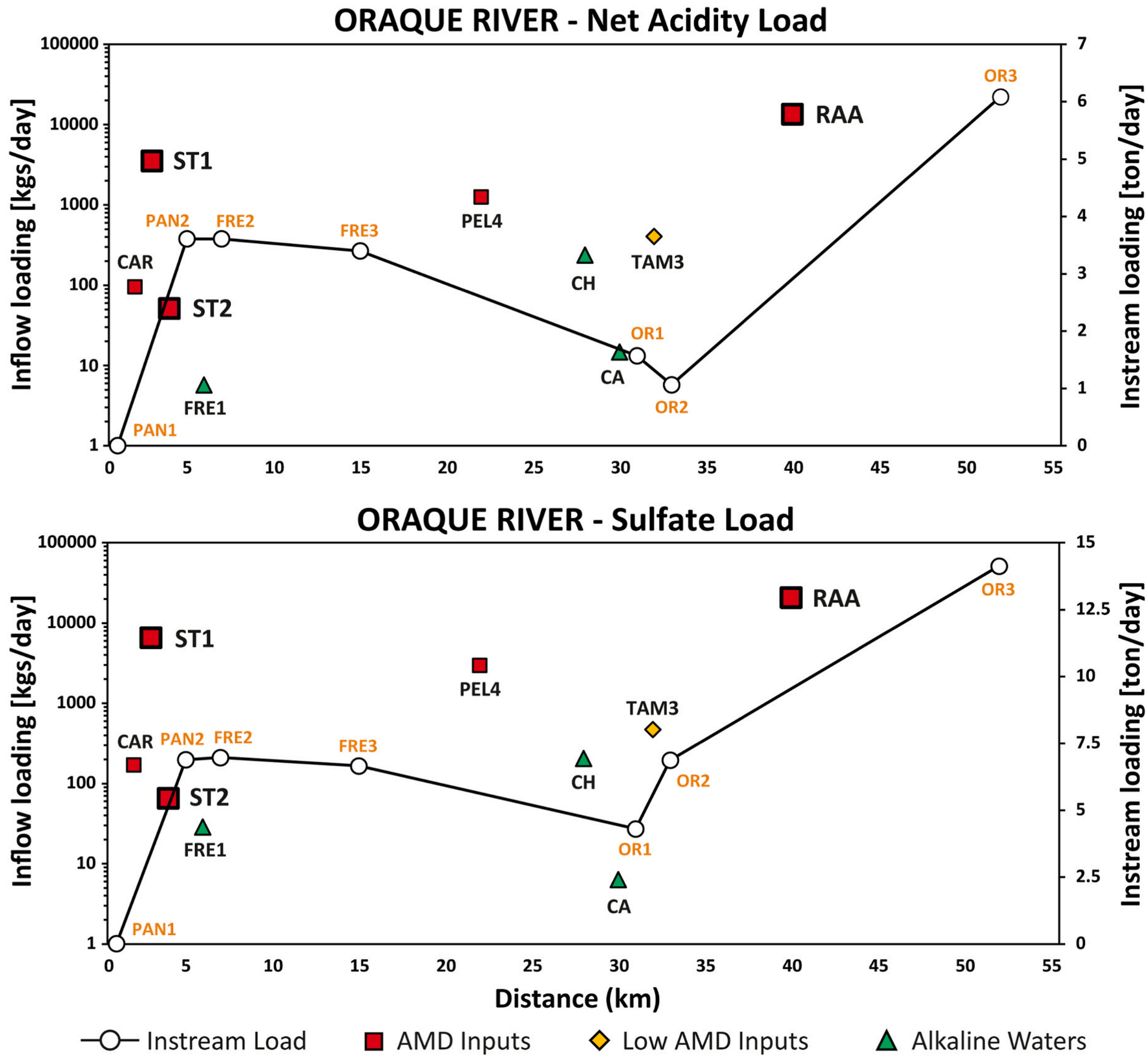

Fig. 4. (*continued*).

difference of −57.6 %) (Fig. S6A and Table S8A), accompanied by a decrease in the modeled pH values, as more intense Fe hydrolysis releases more protons than in the previous model. On the other hand, adjusting the $logK_{sp}$ for each mixture constrains the modeled values to the observed values (average difference of −0.14 %) (Fig. S6B and Table S8B). In fact, using the observed pH values for calculating the $logK_{sp}$ (Caraballo et al., 2013; Schoepfer and Burton, 2021) results in similar solubility constants as the variable approach used for each mixture. Most of them are in the solubility "window" initially proposed by Bigham et al. (1996) and corroborated by others (Sánchez-España et al., 2011; Caraballo et al., 2013). However, in those cases where Fe and sulfate concentrations are higher and pH values are lower, the $logK_{sp}$ decreases (i.e., a lower solubility), approaching the theoretical value of 8.9 calculated thermodynamically by Majzlan et al. (2004) (**see PAN2 and FRE2 in** Table S8B). This assessment of different $logK_{sp}$ values evidences the sensitivity of model outcomes to schwertmannite solubility at basin-scale.

The Fe speciation also has a significant impact on the modeling of these mixtures, as the availability of Fe(III), determined by the kinetics of Fe biotic and abiotic oxidation in acidic waters (Nordstrom, 1985; Sánchez-España et al., 2007), will affect the magnitude of Fe hydrolysis and precipitation processes. When forced to reach atmospheric equilibrium, Fe will undergo oxidation in the modeled mixtures until reaching equilibrium with oxygen, sometimes completely oxidizing Fe (II) to Fe(III), which may lead to overestimate Fe precipitation in some modeled mixtures. However, this process does not occur entirely, evidenced by the remaining presence of Fe(II) throughout the AMD watercourses (**see Fe speciation for February 2023 in** Table S2). Execution of the mixing model without applying atmospheric equilibrium revealed an overestimation of Fe(II) in the confluences compared to the measured values by Fe speciation method (also Fe speciation via PHREEQC calculations) (Fig. S7). This observation may reflect that some of the Fe(II) is being oxidized within mixing zones, showing the importance of using atmospheric equilibrium in the model. Additionally, Sánchez-España et al. (2007) showed that Fe(II) oxidation processes in AMD waters of the IPB are slightly faster than schwertmannite precipitation, as has also been observed in other acidic waters (Nordstrom, 2011), so that the latter would be the limiting reaction. Even though there could be some overestimation of modeled Fe(III) concentration due to forced oxidation, ultimately schwertmannite equilibrium processes would have a greater effect on Fe modeled concentrations.

Iron colloids passing through 0.45 μm filters can lead to overestimating concentrations and saturation indexes in geochemical modeling (Nordstrom, 2011; Nordstrom and Campbell, 2014; Ryskie et al., 2024). Iron speciation for February 2023 showed higher Fe(III)/Fe (II) ratios than those calculated by PHREEQC speciation with measured Eh values (Fig. S8A). These differences could be related to discrepancies

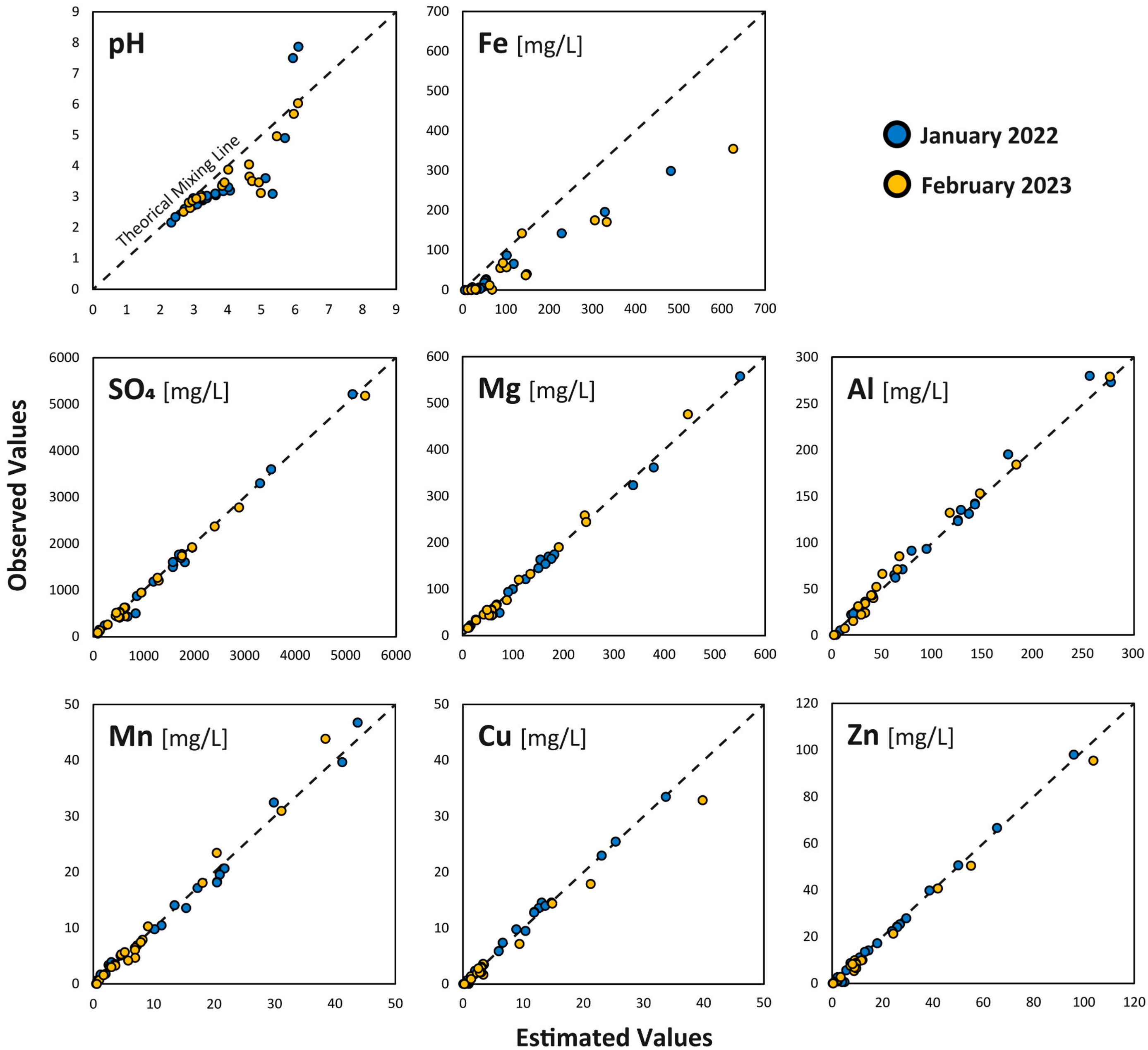

Fig. 5. Comparison between observed and estimated values using the calculated mixing ratios by the mass-balance approach. Sulfate and Mg were used to calculate mixing ratios. No geochemical processes (i.e. mineral equilibrium) were applied on PHREEQC in order to evaluate conservative behavior of constituents. Refer to Fig. 6 for coupled geochemical processes. The dash line indicated the theorical mixing line between end-members.

between measured Eh values and insitu Fe speciation, leading to decreasing the Fe(III)/Fe(II) ratio in PHREEQC speciation calculations when using measured Eh values, probably due to redox pairs imbalance (Appelo and Postma, 2005). However, Eh calculated values using the Fe redox pair (i.e., field Fe speciation) yielded similar values as measured Eh, within an error of 50 mV (Fig. S8B). Otherwise, there could be some interference of iron colloids with field Fe speciation, or PHREEQC speciation calculations related to redox imbalance. Future work assessing these discrepancies between field and PHREEQC speciation would be helpful for improving modeling results.

3.4. Pollutant loads reduction simulations

A model that includes the *wateq4f.dat* database and the schwertmannite solubility constant from Bigham et al. (1996) (i.e. $\log K_{sp} = 18 \pm 2.5$) will serve as the basis for modeling the potential restoration measurements in the priority sites (i.e., Riotinto, San Telmo and Tharsis mines) of the Odiel basin. Two different scenarios are considered: i) a 50 % and ii) 100 % reduction of AMD generated in these mine sites. Supplementary Material provides further details on how these pollution reduction scenarios (50 % and 100 % cases) were implemented in the mixing model (Table S9). Table 1 presents the different simulation results for both sampling campaigns at the Alcolea site. Since water quality recommendations are based on concentrations of constituents (irrigation water: Ayers and Westcot, 1985; drinking water: World Health Organization, 2022; European Council, 2020), only those will be discussed in this section, although mass loadings will still be available in Table S9.

In the January 22 model, the 50 % reduction scenario would result in a notable decline of the net acidity (NA) from a modeled value of 493 to

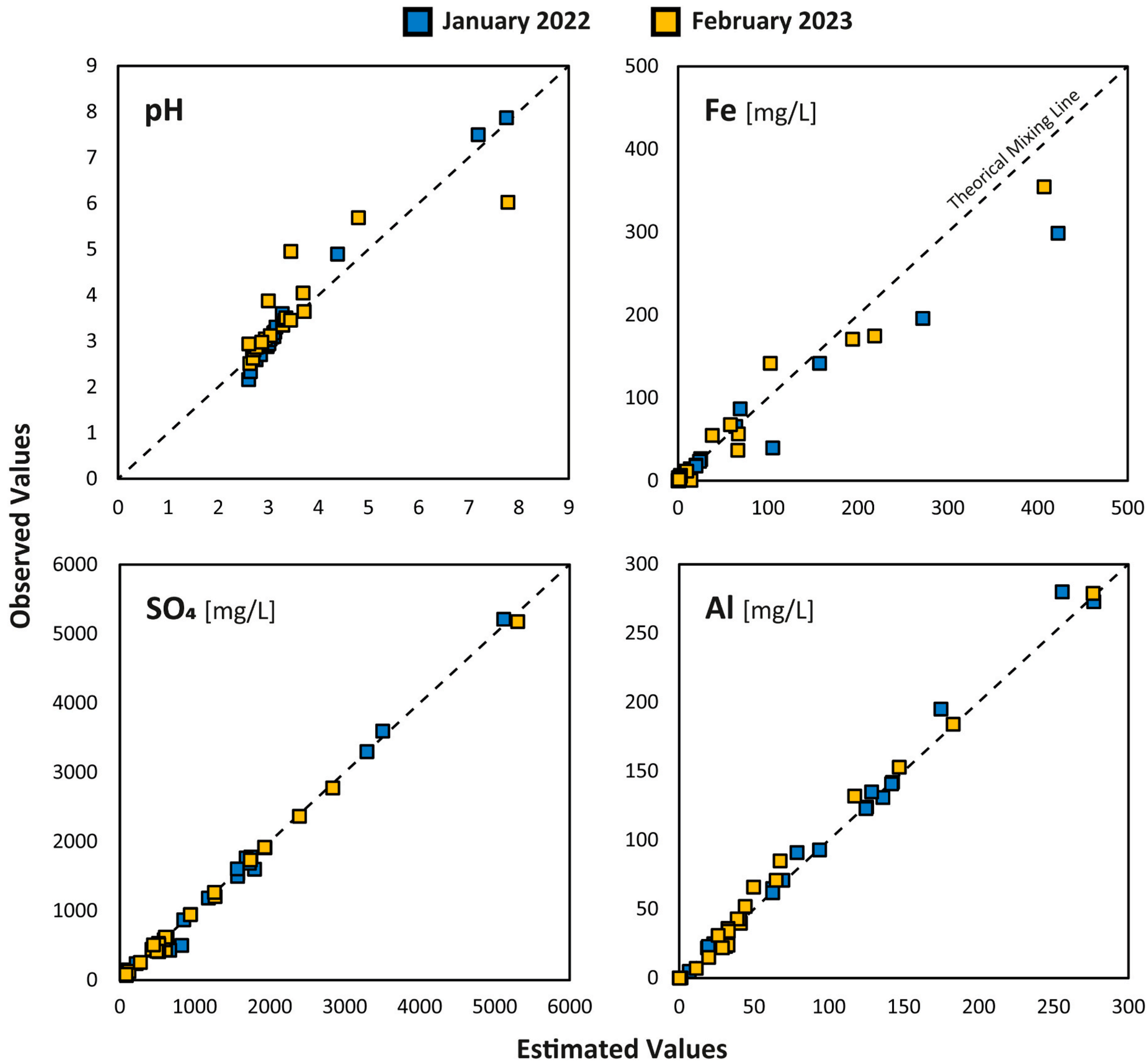

Fig. 6. Equilibrium-coupled mixing model estimated values compared to observed values. Equilibrium reactions for schwertmannite, basaluminite, gypsum and the atmosphere were added to PHREEQC mixing calculations.

252 mg/L eq. $CaCO_3$ and slightly increased pH from 3.10 to 3.39, thereby improving the receiving water quality. The 100 % reduction scenario would lead to an improvement in water quality with 8.75 mg/L eq. $CaCO_3$ of NA and a pH of 4.93. The latter is mostly below the water guidelines restrictions for drinking and irrigation purposes. However, Mn concentration exceeds both limits, Cu is above the limit for irrigation water and Fe is only exceeding the EU regulations. Nevertheless, Mn and Cu may be sorbed or coprecipitated with Fe and Al mineral phases in a real case scenario (Webster et al., 1998; Paulson and Balistrieri, 1999; Nordstrom, 2011; Carrero et al., 2015), potentially reducing these values below the recommended limits. Iron may also be expected to have lower concentration values in a real case, since the estimated starting concentration (i.e., 9.14 mg/L), and then used for simulations, is higher than that observed at the site (i.e., 5.97 mg/L). Notably, the pH value remains acidic even after the total elimination of the three most pollutant sources along the basin, underscoring the considerable acidity potential posed by minor mine discharges and other sources (Figs. 3 and 4).

Specially for the February 2023 model, estimated values are comparably higher than observed (Table 1), indicating that the model tends to overestimate concentrations in high-flow conditions. Consequently, the predicted water quality improvements are likely underestimated, as real conditions would likely show lower constituents concentrations than those used in the simulations. The 50 % reduction simulation reduces the NA from a modeled value of 233 to 205 mg/L eq. $CaCO_3$ and slightly increases pH from 3.35 to 3.41. This improvement is significantly less than the 50 % case for January 22, which may be due to Fe and Al hydrolysis buffering the system (Cánovas et al., 2007; Nordstrom, 2011) or other AMD sources contributing more acidity due to the higher flows and loads (see inflow loadings in Figs. 3 and 4 compared to **3S and 4S**). The 100 % removal simulation estimates a better water quality than the January 2022 simulation, with the NA decreasing to 4.63 mg/L eq. $CaCO_3$ and pH increasing to 7.64. Higher flows recorded on February 2023 would likely neutralize and dilute minor AMD discharges more effectively due to increased clean and alkaline waters fluxes, unlike January 2022, when lower river levels with less neutralization potential would amplify the effect of acidic discharges (i.e. others than those eliminated in this 100 % scenario). Manganese and Cu are still slightly above the acceptable limits, but as mentioned before a real case scenario would likely yield better conditions of water quality. In this case, pH is circumneutral, falling within the range of suitable water for drinking and irrigation purposes.

The results clearly show that reclamation of the basin must be adequate to achieve proper water goals, as even with a substantial 50 % reduction in the pollutant loads of these major sources, the acidity and metal concentrations would remain above water quality guidelines,

Table 1
Pollutant load reductions simulations results for the OD9 sampling point (Fig. 3) where the Alcolea Reservoir is projected to be located (Fig. 1). The modified geochemical equilibrium model (Fe and Al) is applied here. World Health Organization (WHO) guidelines for drinking waters (World Health Organization, 2022), Food and Agriculture Organization (FAO) of the United States guidelines for irrigation waters (Ayers and Westcot, 1985) and European Union (EU) guidelines for drinking waters (European Council, 2020). n.g.: No guideline.

January 2022								
OD9 - Alcolea Reservoir		Al	Cu	Fe	Mn	Zn	Sulfate	Net Acidity
	pH	[mg/L]						[mg/L eq. CaCO3]
Observed Values	3.18	70.6	7.43	5.97	10.5	14.1	949	489
Estimated Values	3.10	69.1	6.60	9.14	11.3	14.4	943	493
50 % Reduction Scenario	3.39	35.9	3.58	1.56	6.49	7.85	549	252
100 % Reduction Scenario	4.93	0.02	0.60	0.64	1.78	1.78	163	8.75
WHO	6.50–8.50	0.90	2.00	n.g.	0.08	3.00	500	–
FAO	6.50–8.40	5.00	0.20	5.00	0.20	2.00	1000	–
EU	6.50–9.50	0.20	2.00	0.20	0.05	n.g.	250	–
February 2023								
OD9 - Alcolea Reservoir		**Al**	**Cu**	**Fe**	**Mn**	**Zn**	**Sulfate**	**Net Acidity**
	pH	**[mg/L]**						**[mg/L eq. CaCO3]**
Observed Values	3.51	21.6	2.07	2.84	4.23	6.8	422	162
Estimated Values	3.35	28.7	4.94	1.95	10.0	14.4	490	234
50 % Reduction Scenario	3.41	28.2	2.64	1.39	5.49	7.57	473	205
100 % Reduction Scenario	7.64	0.04	0.37	0.00	1.03	1.25	124	4.63
WHO	6.50–8.50	0.90	2.00	n.g.	0.08	3.00	500	–
FAO	6.50–8.40	5.00	0.20	5.00	0.20	2.00	1000	–
EU	6.50–9.50	0.20	2.00	0.20	0.05	n.g.	250	–

reflecting the enormous effect of AMD in the region.

4. Environmental management of AMD-affected catchments

The model indicated that reductions in AMD generation ranging from 50 to 100 % should be achieved in the three main AMD sources within the Odiel River to attain a good water quality. These reductions should be accomplished by the implementation of cost-effective measures. Remediation strategies can be divided into preventive and AMD treatment technologies. Nowadays, government regulations mandate operating mines to apply proper management of their mining project to actively prevent the formation of mine discharges. However, historical mine sites in the IPB mostly lack these prevention methods and administrations need to design specific methods for each site. The most commonly used prevention methods include the diversion of surface water by means of perimeter channels (Cánovas et al., 2018b), or the sealing of mine adits and shafts by applying controlled bulkheads (Walton-Day et al., 2021), however, the latter could fail and produce deleterious consequences (Nordstrom and Alpers, 1999; Olías et al., 2019). The goal is reducing the contact of clean waters with sulfides and, therefore, decreasing the pollutant loads generated. Other methods are based on “dry covers” (Cánovas et al., 2019), “wet covers” (Swanson et al., 1997), mine wastes microencapsulation (Tu et al., 2022) and blending of mine wastes with alkaline materials (Pérez-López et al., 2007; Fernández-Caliani and Barba-Brioso, 2010). Technologies are differentiated between active and passive treatment plants. Active treatment technologies require continuous consumption of energy and reagents, as well as intrinsic process control, making them ideal for active mines in the IPB (Macías et al., 2017a). Passive treatment technologies are adequate for abandoned mine sites since they take advantage of natural processes, require no energy consumption and their maintenance is sporadic. However, common passive technologies (e.g., wetlands, anoxic limestone drains, reducing and alkalinity producing systems, etc.) have resulted non-effective for treating the IPB leachates owing to their extreme acidity and metal contents (inducing quick passivation and clogging related to Fe and Al precipitation). In this regard, the Dispersed Alkaline Substrate (DAS) technology is especially designed to treat these leachates and has been successfully applied in the full-scale plants of Esperanza and Concepción mines, with a great efficiency in the removal of metals and acidity (Macías et al., 2012; Orden et al., 2021; Guerrero et al., 2024). However, this technology is designed for low-medium flows (up to 5 L/s), hence in AMD sources exceeding these flows, a flow regulation system or the application of active treatments is needed instead (Caraballo et al., 2016). The combination of the abovementioned preventive and remediation measures, either active or passive treatments, in the main AMD generating mine sites (i.e., Riotinto, San Telmo and Tharsis) within the Odiel basin can help achieve the proposed AMD reduction goals, and therefore to obtain waters suitable for use. Furthermore, mine waters have been established as a potential secondary source of base, industrial and technology metals (Orden et al., 2021; León et al., 2021).

The following specific proposals derive from the main findings of this study. According to mass loadings assessment, the Riotinto Minging District is of great concern due to the high flow rates generated within the drainage basin of the Agrio Creek, limiting the feasibility of passive treatments. The mine is currently operating and making efforts to address its environmental liabilities. Preventive measures, such as sealing mine adits, diverting rainwater into perimeter channels, and regulating pit water levels to avoid overflow, have successfully minimized the interaction between surface runoff and mine wastes. As a result, pollutant loads discharged into the Odiel River have been reduced (León et al., 2023). In addition to these measures, a treatment strategy combining DAS plants for low-flow or stable discharges (<5 L/s) during dry periods with active treatment systems designed to manage the large AMD volumes typical of the rainy season could be beneficial. Recently, the application of technosols to Riotinto mine wastes/soils have proven effective in mitigating the acidity and metal release (Santos et al., 2019; Fernández-Caliani et al., 2024), making this a promising complementary measure to manage direct precipitation over waste dumps.

Reclamation of the Tharsis Mining District is particularly challenging due to the large volume of spoil heaps that generate highly concentrated leachates intro the Meca and Oraque sub-basins (Moreno-González et al., 2020, 2022). Given the current importance of the Alcolea Reservoir (in 2025), remediation efforts should prioritize areas draining into the Oraque River (or Aguas Agrias Creek). Currently, the construction of DAS plants could be considered for low-flow discharges; however, spatial constraints in certain zones limit their feasibility, requiring relocation downstream where higher flow rates are present (Moreno-González et al., 2020, 2022). During the rainy season, the increase in flows (>5L/s) would render DAS plants as unsuitable. Besides, diffuse inputs from large sulfide dumps add complexity to the system. Therefore, priority should be given to preventing runoff water from contacting the sulfide piles, thereby decreasing flows of the leachate generated, followed by measures to inhibit pyrite oxidation to limit acidity and metals release. In this sense, Castellanos-Vásquez et al. (2025), using microencapsulation, and Diosdado-Aragón et al., (2025), through mixing with alkaline industrial residues, have obtained promising results in mitigating the AMD production from massive sulfides of the IPB. Therefore, the hybrid DAS-active treatment strategy would be a suitable remediation measure for this site. In addition, recent research suggests recycling and recovering critical raw material from spoil heaps (Cánovas et al., 2021; Rosario-Beltré et al., 2023; Yesares et al., 2023), which may partially offset remediation costs by reducing the initial investment required. The recent acquisition and exploration of the Tharsis mines by a mining consortium could represent an opportunity for substantial environmental improvements, as the company is legally required to assume existing environmental liabilities prior to resuming operations.

The San Telmo mine is drained by two small creeks that converge into the Panera Creek, tributary of the Oraque River. The main creek receives leachates from both the NE and W dumps, linking them through a pit-lake flow-through system (Fuentes-López et al., 2022). Restoration efforts should prioritize preventing inflows into the pit lake, which would otherwise raise its water level and cause overflow toward the W dumps, increasing the main creek discharge. Installing perimeter channels could reduce runoff in contact with the NE dumps, limiting pit-lake inputs and thus potentially lowering pollutant loads. Diverting clean water around the mine and reconnecting it downstream of the main creek would further dilute contaminant concentrations. The reduced flows near the W dumps would create suitable conditions for implementing DAS plants. To improve efficiency during high-flow periods, constructing diversion channels to evenly distribute water across multiple DAS plants may be the most appropriate method, thereby enhancing pollution control. Additionally, measures aimed at reducing acid generation from the W dumps, identified as the most critical pollution source (Fuentes-López et al., 2022), are worth testing, including some of the preventive approaches described above.

5. Conclusions

This study quantifies the mass loads transported towards the future Alcolea Reservoir, projected to be constructed in the Odiel River basin, and predicts through geochemical modeling the post-reclamation water quality. Under average flow conditions, the Odiel River would transport high amounts of net acidity (54.0 tons/day), sulfate (105 tons/day) and dissolved metals (11.6 tons/day of Fe, Al, Mn, Cu and Zn). During high flows, dissolved loads are predicted to decrease by 21.3 % of net acidity and 18.0 % of dissolved metals, as a response to naturally occurring neutralizing and precipitation processes, generally consistent with winter-spring high-flow periods, while sulfate increases by 5.66 % due to its more conservative behavior. Mass loading estimations identified the Riotinto, Tharsis and San Telmo mines, as main contributors of pollution in the drainage area; accounting for 64.4 %, 18.7 % and 5.93 % of net acidity load on January 2022; and 77.1 %, 9.00 % and 4.14 % on February 2023; respectively. Installation of gauging stations throughout the basin is strongly recommended to facilitate monitoring seasonal and climate-driven variations in mass loadings.

The mixing model developed for the two study periods effectively reproduces the geochemical changes in surface waters caused by AMD inputs into the Odiel River. Some reliability issues have emerged regarding non-conservative constituents (mainly pH, Fe, Al, and to a lesser extent Cu). The solubility constant of schwertmannite seems to be the most influential factor in the estimations, as variations in the constant dictate Fe precipitation on mixing processes, subsequently altering pH through Fe hydrolysis. The schwertmannite "solubility window" proposed previously by some authors ($logK_{sp}$ from 5.8 to 39.5) provides estimations of Fe and pH across diverse catchment conditions. While the model assumes equilibrium, Fe precipitation is kinetically controlled at basin scale and may not be attained at certain mixing points (e.g., upper Oraque sub-basin), making the solubility range useful for adjusting non-equilibrated waters. Further research should aim to study Fe precipitation kinetics at the scale of the Odiel River basin. Additional constraints such as Fe(III)/Fe(II) ratios, coprecipitation/sorption of metals onto Fe minerals, spatial sampling uncertainties and the consistency of the thermodynamic database used could also have an impact on model reliability. Traditionally used *wateq4f* database from Ball and Nordstrom (1991) and schwertmannite $logK_{sp} = 18 \pm 2.5$ from Bigham et al. (1996) in the acid mine drainage literature have yielded the best modeling results in this study.

A modified equilibrium-based mixing model was used to simulate pollutant load reductions for the three main AMD sources. Full reclamation would significantly improve water quality at the Alcolea Reservoir site, with net acidity decreasing to 8.75 mg/L (eq. $CaCO_3$) and pH rising to 4.93 in January 2022, and to 4.63 mg/L and 7.64 in February 2023, thus complying with water guidelines (with slight exceedances for Mn and Cu). Besides, since it was first developed on a conservative approach (i.e., underestimated removal for constituents with non-coupled geochemical processes, such as sorption or coprecipitation), potential water improvements (e.g., Mn and Cu) might be even greater than, or at least comparable to, those presented above. Nonetheless, the model also underscores that the restoration measures must be effective, given that in a 50 % reduction scenario, the water quality is still far from meeting water guidelines.

CRediT authorship contribution statement

Jonatan Romero-Matos: Writing – review & editing, Writing – original draft, Visualization, Methodology, Data curation, Conceptualization. **Laura Sánchez-López:** Writing – review & editing, Methodology, Data curation. **Rafael León:** Writing – review & editing, Methodology, Data curation. **Robert L. Runkel:** Writing – review & editing, Validation. **D. Kirk Nordstrom:** Writing – review & editing, Validation, Formal analysis. **Carlos R. Cánovas:** Writing – review & editing, Supervision, Investigation, Funding acquisition, Conceptualization. **Francisco Macías:** Writing – review & editing, Supervision, Investigation, Conceptualization. **José Miguel Nieto:** Writing – review & editing, Supervision, Project administration, Funding acquisition, Conceptualization.

Declaration of competing interest

The authors declare that they have no known competing financial interests or personal relationships that could have appeared to influence the work reported in this paper.

Acknowledgments

This research was supported by the the Spanish Ministry of Science, Innovation and Universities under the research project DYNAMICO (PID2023-151504OB-I00) funded by MICIU/AEI/10.13039/501100011033. This work was also supported by the I+D+ i ERA-MIN3 SuMRee project (PCI2024-153500) funded by MICIU/AEI/10.13039/501100011033, and by the European Union NextGenerationEU/PRTR. L. Sánchez-López acknowledges the "Formación de Personal Investigador" grant (PRE2021-097651) funded by MCIN/AEI/10.13039/501100011033. C.R Cánovas thanks the Spanish Ministry of Science and Innovation for the Postdoctoral Fellowship granted under application reference RYC 2019-027949-I funded by MCIN/AEI/10.13039/501100011033. J. Romero-Matos is financed by a FPU program of the Spanish Ministry of Education and Vocational Training (FPU20/04441). Rob Runkel's participation in this project was funded by the U.S. Geological Survey (USGS) through the Environmental Health Program of the Ecosystems Mission Area. All data collection and laboratory analyses are presented in this manuscript and supplement. Additional information may be obtained by contacting the corresponding author. Any use of trade, firm, or product names is for descriptive purposes only and does not imply endorsement by the U.S. Government. We thank Dr. Carleton Bern from the USGS for comments on an early version of this manuscript. The authors gratefully appreciate the constructive comments and suggestions from the associate editor and three anonymous reviewers. Funding for open access charge: Universidad de Huelva/CBUA.

Appendix A. Supplementary data

Supplementary data associated with this article can be found, in the online version, at https://doi.org/10.1016/j.jenvman.2025.127486.

Data availability

Data will be made available on request.

References

Appelo, C.A.J., Postma, D., 2005. Geochemistry, Groundwater and Pollution, 2nd. Balkema, Leiden, p. 678. https://doi.org/10.1201/9781439833544.

Ayers, R.S., Westcot, D.W., 1985. Water quality for agriculture (Vol. 29, p. 174). Rome. Food and agriculture organization of the United Nations. https://www.fao.org/4/t0234e/T0234E00.htm#TOC.

Ayora, C., Caraballo, M.A., Macías, F., Rötting, T.S., Carrera, J., Nieto, J.M., 2013. Acid mine drainage in the Iberian Pyrite Belt: 2. Lessons learned from recent passive remediation experiences. Environ. Sci. Pollut. Control Ser. 20, 7837–7853. https://doi.org/10.1007/s11356-013-1479-2.

Balistrieri, L.S., Seal II, R.R., Piatak, N.M., Paul, B., 2007. Assessing the concentration, speciation, and toxicity of dissolved metals during mixing of acid-mine drainage and ambient river water downstream of the Elizabeth Copper Mine, Vermont, USA. Appl. Geochem. 22 (5), 930–952. https://doi.org/10.1016/j.apgeochem.2007.02.005.

Ball, J.W., Nordstrom, D.K., 1991. User's manual for WATEQ4F, with revised thermodynamic data base and text cases for calculating speciation of major, trace, and redox elements in natural waters (No. 91-183). US Geological Survey. https://doi.org/10.3133/ofr91183.

Ball, J.W., Runkel, R.L., Nordstrom, D.K., 2004. Evaluating remedial alternatives for the Alamosa River and Wightman Fork, near Summitville Mine, Colorado: application of a reactive transport model to low-and high-flow simulations. https://pubs.usgs.gov/publication/70199402.

Bigham, J.M., Nordstrom, D.K., 2000. Iron and aluminum hydroxysulfates from acid sulfate waters. Rev. Mineral. Geochem. 40 (1), 351–403. https://doi.org/10.2138/rmg.2000.40.7.

Bigham, J.M., Schwertmann, U., Traina, S.J., Winland, R.L., Wolf, M., 1996. Schwertmannite and the chemical modeling of iron in acid sulfate waters. Geochem. Cosmochim. Acta 60 (12), 2111–2121. https://doi.org/10.1016/0016-7037(96)00091-9.

Cánovas, C.R., Olías, M., Nieto, J.M., Sarmiento, A.M., Cerón, J.C., 2007. Hydrogeochemical characteristics of the Tinto and Odiel Rivers (SW Spain). Factors controlling metal contents. Sci. Total Environ. 373 (1), 363–382. https://doi.org/10.1016/j.scitotenv.2006.11.022.

Cánovas, C.R., Olías, M., Sarmiento, A.M., Nieto, J.M., Galván, L., 2012. Pollutant transport processes in the Odiel River (SW Spain) during rain events. Water Resour. Res. 48 (6). https://doi.org/10.1029/2011WR011041.

Cánovas, C.R., Olías, M., Macías, F., Torres, E., San Miguel, E.G., Galván, L., Ayora, C., Nieto, J.M., 2016. Water acidification trends in a reservoir of the Iberian Pyrite Belt (SW Spain). Sci. Total Environ. 541, 400–411. https://doi.org/10.1016/j.scitotenv.2015.09.070.

Cánovas, C.R., Macías, F., Olías, M., López, R.P., Nieto, J.M., 2017. Metal-fluxes characterization at a catchment scale: study of mixing processes and end-member analysis in the Meca River watershed (SW Spain). J. Hydrol. 550, 590–602. https://doi.org/10.1016/j.jhydrol.2017.05.037.

Cánovas, C.R., Riera, J., Carrero, S., Olías, M., 2018a. Dissolved and particulate metal fluxes in an AMD-affected stream under different hydrological conditions: the Odiel River (SW Spain). Catena 165, 414–424. https://doi.org/10.1016/j.catena.2018.02.020.

Cánovas, C.R., Macías, F., Olías, M., 2018b. Hydrogeochemical behavior of an anthropogenic mine aquifer: implications for potential remediation measures. Sci. Total Environ. 636, 85–93.

Blowes, D.W., Ptacek, C.J., Jambor, J.L., Weisener, C.G., Paktunc, D., Gould, W.D., Johnson, D.B., 2014. The geochemistry of acid mine drainage. In: Treatise on Geochemistry, second ed. https://doi.org/10.1016/B978-0-08-095975-7.00905-0

Cánovas, C.R., Caro-Moreno, D., Jiménez-Cantizano, F.A., Macías, F., Pérez-López, R., 2019. Assessing the quality of potentially reclaimed mine soils: environmental implications for the construction of a nearby water reservoir. Chemosphere 216, 19–30. https://doi.org/10.1016/j.chemosphere.2018.09.018.

Cánovas, C.R., Macías, F., Basallote, M.D., Olías, M., Nieto, J.M., Pérez-López, R., 2021. Metal (loid) release from sulfide-rich wastes to the environment: the case of the Iberian Pyrite Belt (SW Spain). Current Opinion in Environmental Science & Health 20, 100240. https://doi.org/10.1016/j.coesh.2021.100240Caraballo.

Caraballo, M.A., Macías, F., Nieto, J.M., Ayora, C., 2016. Long term fluctuations of groundwater mine pollution in a sulfide mining district with dry Mediterranean climate: implications for water resources management and remediation. Sci. Total Environ. 539, 427–435. https://doi.org/10.1016/j.scitotenv.2015.08.156.

Caraballo, M.A., Rimstidt, J.D., Macías, F., Nieto, J.M., Hochella Jr., M.F., 2013. Metastability, nanocrystallinity and pseudo-solid solution effects on the understanding of schwertmannite solubility. Chemical Geology 360, 22–31. https://doi.org/10.1016/j.chemgeo.2013.09.023.

Carrero, S., Pérez-López, R., Fernandez-Martinez, A., Cruz-Hernández, P., Ayora, C., Poulain, A., 2015. The potential role of aluminium hydroxysulphates in the removal of contaminants in acid mine drainage. Chem. Geol. 417, 414–423. https://doi.org/10.1016/j.chemgeo.2015.10.020.

Castellanos-Vásquez, M., Cánovas, C.R., Macías, F., Nieto, J.M., 2025. Microencapsulation of sulfide mining waste: a strategy for pollution prevention and acid mine drainage mitigation. In: Goldschmidt 2025 Conference. GOLDSCHMIDT. https://conf.goldschmidt.info/goldschmidt/2025/meetingapp.cgi/Paper/29470.

Cravotta III, C.A., 2021. Interactive PHREEQ-N-AMDTreat water-quality modeling tools to evaluate performance and design of treatment systems for acid mine drainage. Appl. Geochem. 126, 104845. https://doi.org/10.1016/j.apgeochem.2020.104845.

Davis, R.A., Welty, A.T., Borrego, J., Morales, J.A., Pendon, J.G., Ryan, J.G., 2000. Rio Tinto estuary (Spain): 5000 years of pollution. Environmental Geology 39, 1107–1116. https://doi.org/10.1007/s002549900096.

Diosdado-Aragón, A.J., Davila, J.M., Caraballo, M.A., 2025. Chemical stability and environmental characterization of alkali-activated mine tailings generated using a MgCO3/MgO industrial residue. J. Geochem. Explor., 107886 https://doi.org/10.1016/j.gexplo.2025.107886.

Dirección General de Infraestructuras del Agua, 2024. Sistema Automático de Información Hidrológica (SAIH Hidrosur). Consejería de Agricultura, Pesca, Agua y Desarrollo Rural de la. Junta de Andalucía. http://www.redhidrosurmedioambiente.es/saih/.

Elghali, A., Benzaazoua, M., Taha, Y., Amar, H., Ait-khouia, Y., Bouzahzah, H., Hakkou, R., 2023. Prediction of acid mine drainage: where we are. Earth Sci. Rev. 241, 104421. https://doi.org/10.1016/j.earscirev.2023.104421.

European Council, 2000. Directive 2000/60/EC of the European Parliament and of the Council of 23 October 2000 establishing a framework for Community action in the field of water policy. Official Journal of the European Communities, L 327, 1–84. http://data.europa.eu/eli/dir/2000/60/oj.

European Council, 2020. Directive (EU) 2020/2184 of the European Parliament and of the Council of 16 December 2020 on the quality of water intended for human consumption. Official Journal of the European Communities, L 435, 1–62. http://data.europa.eu/eli/dir/2020/2184/oj.

Fernández-Caliani, J.C., Barba-Brioso, C., 2010. Metal immobilization in hazardous contaminated minesoils after marble slurry waste application. A field assessment at the Tharsis mining district (Spain). J. Hazard Mater. 181 (1–3), 817–826. https://doi.org/10.1016/j.jhazmat.2010.05.087.

Fernández-Caliani, J.C., Fernández-Landero, S., Giráldez, M.I., Hidalgo, P.J., Morales, E., 2024. Unveiling a Technosol-based remediation approach for enhancing plant growth in an iron-rich acidic mine soil from the Rio Tinto Mars analog site. Sci. Total Environ. 922, 171217. https://doi.org/10.1016/j.scitotenv.2024.171217.

Foulds, S.A., Brewer, P.A., Macklin, M.G., Haresign, W., Betson, R.E., Rassner, S.M.E., 2014. Flood-related contamination in catchments affected by historical metal mining: an unexpected and emerging hazard of climate change. Sci. Total Environ. 476, 165–180. https://doi.org/10.1016/j.scitotenv.2013.12.079.

Fuentes-López, J.M., Olías, M., León, R., Basallote, M.D., Macías, F., Moreno-González, R., Cánovas, C.R., 2022. Stream-pit lake interactions in an abandoned mining area affected by acid drainage (Iberian Pyrite Belt). Science of the Total Environment 833, 155224. https://doi.org/10.1016/j.scitotenv.2022.155224.

Galván, L., Olías, M., Cánovas, C.R., Sarmiento, A.M., Nieto, J.M., 2016. Hydrological modeling of a watershed affected by acid mine drainage (Odiel River, SW Spain).

Assessment of the pollutant contributing areas. J. Hydrol. 540, 196–206. https://doi.org/10.1016/j.jhydrol.2016.06.005.

Guerrero, J.L., León, R., Cánovas, C.R., Pérez-López, R., Nieto, J.M., Macías, F., 2024. First full-scale application of barium carbonate as an effective dispersed alkaline substrate for sulfate removal from acid mine drainage. Sci. Total Environ. 955, 176877. https://doi.org/10.1016/j.scitotenv.2024.176877.

Kefeni, K.K., Msagati, T.A., Mamba, B.B., 2017. Acid mine drainage: prevention, treatment options, and resource recovery: a review. J. Clean. Prod. 151, 475–493. https://doi.org/10.1016/j.jclepro.2017.03.082.

Kimball, B.A., Walton-Day, K., Runkel, R.L., 2007. Quantification of metal loading by tracer injection and synoptic sampling, 1996-2000, chap. E9 of Church, S.E. In: von Guerard, P., Finger, S.E. (Eds.), Integrated Investigations of Environmental Effects of Historical Mining in the Animas River Watershed, San Juan County, Colorado. U.S. Geological Survey Professional Paper 1651, pp. 417–495. https://pubs.usgs.gov/pp/1651/.

Kirby, C.S., Cravotta III, C.A., 2005b. Net alkalinity and net acidity 2: practical considerations. Appl. Geochem. 20 (10), 1941–1964. https://doi.org/10.1016/j.apgeochem.2005.07.003.

Kirby, C.S., Cravotta III, C.A., 2005a. Net alkalinity and net acidity 1: theoretical considerations. Appl. Geochem. 20 (10), 1920–1940. https://doi.org/10.1016/j.apgeochem.2005.07.002.

León, R., Macías, F., Cánovas, C.R., Pérez-López, R., Ayora, C., Nieto, J.M., Olías, M., 2021. Mine waters as a secondary source of rare earth elements worldwide: the case of the Iberian Pyrite Belt. J. Geochem. Explor. 224, 106742. https://doi.org/10.1016/j.gexplo.2021.106742.

León, R., Romero-Matos, J., Macías, F., Sanjuan, E., Nieto, J.M., 2023. Reducción de los aportes difusos de Drenaje Ácido de Mina de la Mina de Riotinto a las cuencas de los ríos Odiel y Tinto (Huelva). Geogaceta 73, 63–66. https://doi.org/10.55407/geogaceta95136.

Li, L., 2019. Watershed reactive transport. Rev. Mineral. Geochem. 85 (1), 381–418. https://doi.org/10.2138/rmg.2018.85.13.

Lozano, A., Fernández-Martínez, A., Ayora, C., Poulain, A., 2018. Local structure and ageing of basaluminite at different pH values and sulphate concentrations. Chem. Geol. 496, 25–33. https://doi.org/10.1016/j.chemgeo.2018.08.002.

Macías, F., Caraballo, M.A., Nieto, J.M., Rötting, T.S., Ayora, C., 2012. Natural pretreatment and passive remediation of highly polluted acid mine drainage. J. Environ. Manag. 104, 93–100. https://doi.org/10.1016/j.jenvman.2012.03.027.

Macías, F., Pérez-López, R., Caraballo, M.A., Cánovas, C.R., Nieto, J.M., 2017a. Management strategies and valorization for waste sludge from active treatment of extremely metal-polluted acid mine drainage: a contribution for sustainable mining. J. Clean. Prod. 141, 1057–1066. https://doi.org/10.1016/j.jclepro.2016.09.181.

Macías, F., Pérez-López, R., Caraballo, M.A., Sarmiento, A.M., Cánovas, C.R., Nieto, J.M., Olías, M., Ayora, C., 2017b. A geochemical approach to the restoration plans for the Odiel River basin (SW Spain), a watershed deeply polluted by acid mine drainage. Environ. Sci. Pollut. Control Ser. 24, 4506–4516. https://doi.org/10.1007/s11356-016-8169-9.

Majzlan, J., Navrotsky, A., Schwertmann, U., 2004. Thermodynamics of iron oxides: Part III. Enthalpies of formation and stability of ferrihydrite (∼ Fe (OH) 3), schwertmannite (∼ FeO (OH) 3/4 (SO4) 1/8), and ε-Fe2O3. Geochem. Cosmochim. Acta 68 (5), 1049–1059. https://doi.org/10.1016/S0016-7037(03)00371-5.

Millán-Becerro, R., Pérez-López, R., Cánovas, C.R., Macías, F., León, R., 2023. Phosphogypsum weathering and implications for pollutant discharge into an estuary. J. Hydrol. 617, 128943. https://doi.org/10.1016/j.jhydrol.2022.128943.

Moreno-González, R., Cánovas, C.R., Olías, M., Macías, F., 2020. Seasonal variability of extremely metal rich acid mine drainages from the Tharsis mines (SW Spain). Environmental Pollution 259, 113829. https://doi.org/10.1016/j.envpol.2019.113829.

Moreno-González, R., Macías, F., Olías, M., Canovas, C.R., 2022. Temporal evolution of acid mine drainage (AMD) leachates from the abandoned tharsis mine (Iberian Pyrite Belt, Spain). Environmental Pollution 295, 118697. https://doi.org/10.1016/j.envpol.2021.118697.

Mosley, L.M., Daly, R., Palmer, D., Yeates, P., Dallimore, C., Biswas, T., Simpson, S.L., 2015. Predictive modelling of pH and dissolved metal concentrations and speciation following mixing of acid drainage with river water. Appl. Geochem. 59, 1–10. https://doi.org/10.1016/j.apgeochem.2015.03.006.

Nieto, J.M., Sarmiento, A.M., Canovas, C.R., Olias, M., Ayora, C., 2013. Acid mine drainage in the Iberian Pyrite Belt: 1. Hydrochemical characteristics and pollutant load of the Tinto and Odiel rivers. Environ. Sci. Pollut. Control Ser. 20, 7509–7519. https://doi.org/10.1007/s11356-013-1634-9.

Nordstrom, D.K., 1985. The Rate of Ferrous Iron Oxidation in a Stream Receiving Acid Mine Effluent. Selected Papers in the Hydrologic Sciences, pp. 113–119.

Nordstrom, D.K., 2011. Hydrogeochemical processes governing the origin, transport and fate of major and trace elements from mine wastes and mineralized rock to surface waters. Appl. Geochem. 26 (11), 1777–1791. https://doi.org/10.1016/j.apgeochem.2011.06.002.

Nordstrom, D.K., 2012. Models, validation, and applied geochemistry: issues in science, communication, and philosophy. Appl. Geochem. 27 (10), 1899–1919. https://doi.org/10.1016/j.apgeochem.2012.07.007.

Nordstrom, D.K., 2020. Geochemical modeling of iron and aluminum precipitation during mixing and neutralization of acid mine drainage. Minerals 10 (6), 547. https://doi.org/10.3390/min10060547.

Nordstrom, D.K., Alpers, C.N., 1999. Negative pH, efflorescent mineralogy, and consequences for environmental restoration at the Iron Mountain Superfund site, California. Proc. Natl. Acad. Sci. 96 (7), 3455–3462. https://doi.org/10.1073/pnas.96.7.3455.

Nordstrom, D.K., Ball, J.W., 1986. The geochemical behavior of aluminum in acidified surface waters. Science 232 (4746), 54–56. https://doi.org/10.1126/science.232.4746.54.

Nordstrom, D.K., Campbell, K.M., 2014. Modeling low-temperature geochemical processes. Treatise on Geochemistry 7, 27–68. https://doi.org/10.1016/B978-0-08-095975-7.00502-7.

Nordstrom, D.K., Wilde, F.D., 1998. Reduction–oxidation Potential (Electrode Method). National Field Manual for the Collection of Water Quality Data, Book 9, Chapter 6.5. US Geological Survey Techniques of Water-Resources Investigations. US Geological Survey, Reston, VA, p. 20. https://pubs.usgs.gov/publication/twri09A6.5.

Olıas, M., Nieto, J.M., Sarmiento, A.M., Cerón, J.C., Cánovas, C.R., 2004. Seasonal water quality variations in a river affected by acid mine drainage: the Odiel River (South West Spain). Sci. Total Environ. 333 (1–3), 267–281. https://doi.org/10.1016/j.scitotenv.2004.05.012.

Olías, M., Cánovas, C.R., Nieto, J.M., Sarmiento, A.M., 2006. Evaluation of the dissolved contaminant load transported by the Tinto and Odiel rivers (South West Spain). Appl. Geochem. 21 (10), 1733–1749. https://doi.org/10.1016/j.apgeochem.2006.05.009.

Olías, M., Nieto, J.M., Sarmiento, A.M., Cánovas, C.R., Galván, L., 2011. Water quality in the future Alcolea reservoir (Odiel River, SW Spain): a clear example of the inappropriate management of water resources in Spain. Water Resour. Manag. 25, 201–215. https://doi.org/10.1007/s11269-010-9695-8.

Olías, M., Cánovas, C.R., Basallote, M.D., Macías, F., Pérez-López, R., González, R.M., Millán-Becerro, R., Nieto, J.M., 2019. Causes and impacts of a mine water spill from an acidic pit lake (Iberian Pyrite Belt). Environmental Pollution 250, 127–136. https://doi.org/10.1016/j.envpol.2019.04.011.

Orden, S., Macías, F., Cánovas, C.R., Nieto, J.M., Pérez-López, R., Ayora, C., 2021. Eco-sustainable passive treatment for mine waters: full-scale and long-term demonstration. J. Environ. Manag. 280, 111699. https://doi.org/10.1016/j.jenvman.2020.111699.

Papaslioti, E.M., Giampouras, M., Sánchez-López, L., Basallote, M.D., Freydier, R., Cánovas, C.R., Pérez-López, R., 2024. Temporal dynamics of contaminants in an estuarine system affected by acid mine drainage discharges. Sci. Total Environ. 947, 174683. https://doi.org/10.1016/j.scitotenv.2024.174683.

Parkhurst, D.L., Appelo, C.A.J., 2013. Description of input and examples for PHREEQC version 3—a computer program for speciation, batch-reaction, one-dimensional transport, and inverse geochemical calculations. US geological survey techniques and methods 6 (A43), 497. https://doi.org/10.3133/tm6A43.

Paulson, A.J., Balistrieri, L., 1999. Modeling removal of Cd, Cu, Pb, and Zn in acidic groundwater during neutralization by ambient surface waters and groundwaters. Environmental Science & Technology 33 (21), 3850–3856. https://doi.org/10.1021/es9900454.

Pelizardi, F., Bea, S.A., Carrera, J., Vives, L., 2017. Identifying geochemical processes using End Member Mixing Analysis to decouple chemical components for mixing ratio calculations. J. Hydrol. 550, 144–156. https://doi.org/10.1016/j.jhydrol.2017.04.010.

Pérez-López, R., Nieto, J.M., de Almodóvar, G.R., 2007. Immobilization of toxic elements in mine residues derived from mining activities in the Iberian Pyrite Belt (SW Spain): laboratory experiments. Appl. Geochem. 22 (9), 1919–1935. https://doi.org/10.1016/j.apgeochem.2007.03.055.

Pérez-López, R., Millán-Becerro, R., Basallote, M.D., Carrero, S., Parviainen, A., Freydier, R., Macías, F., Cánovas, C.R., 2023. Effects of estuarine water mixing on the mobility of trace elements in acid mine drainage leachates. Mar. Pollut. Bull. 187, 114491. https://doi.org/10.1016/j.marpolbul.2022.114491.

Reisman, D.J., Sundaram, V., Al-Abed, S.R., Allen, D., 2007. Statistical validation of sulfate quantification methods used for analysis of acid mine drainage. Talanta 71 (1), 303–311. https://doi.org/10.1016/j.talanta.2006.04.002.

Remesal, J.A., 2024. Restoration strategy of the Odiel River catchment AMD. In: Proceedings of the XIII Spanish Dams Conference. B.1. Environmental and Social Aspects of Dams and Reservoirs congressarchive.cimne.com/spancold_2024/papers/1b20f8db8df711eea683000c29ddfc0c.pdf.

Rosario-Beltré, A.J., Sánchez-España, J., Rodríguez-Gómez, V., Fernández-Naranjo, F.J., Bellido-Martín, E., Adánez-Sanjuán, P., Arranz-González, J.C., 2023. Critical Raw Materials recovery potential from Spanish mine wastes: a national-scale preliminary assessment. J. Clean. Prod. 407, 137163. https://doi.org/10.1016/j.jclepro.2023.137163.

Rossi, C., Oyarzún, J., Pastén, P., Runkel, R.L., Núñez, J., Duhalde, D., et al., 2021. Assessment of a conservative mixing model for the evaluation of constituent behavior below river confluences, Elqui River Basin, Chile. River Res. Appl. 37 (7), 967–978. https://doi.org/10.1002/rra.3823.

Runkel, R.L., McKnight, D.M., Bencala, K.E., Chapra, S.C., 1996. Reactive solute transport in streams: 2. Simulation of a pH modification experiment. Water Resour. Res. 32 (2), 419–430. https://doi.org/10.1029/95WR03107.

Runkel, R.L., Kimball, B.A., 2002. Evaluating remedial alternatives for an acid mine drainage stream: Application of a reactive transport model. Environmental Science and Technology 36 (5), 1093–1101. https://doi.org/10.1021/es0109794.

Runkel, R.L., Kimball, B.A., Walton-Day, K., Verplanck, P.L., Broshears, R.E., 2012. Evaluating remedial alternatives for an acid mine drainage stream: a model post audit. Environ. Sci. Technol. 46 (1), 340–347. https://doi.org/10.1021/es2038504.

Runkel, R.L., Walton-Day, K., Kimball, B.A., Verplanck, P.L., Nimick, D.A., 2013. Estimating instream constituent loads using replicate synoptic sampling, Peru Creek, Colorado. J. Hydrol. 489, 26–41. https://doi.org/10.1016/j.jhydrol.2013.02.031.

Ryskie, S., Rosa, E., Neculita, C.M., Couture, P., 2024. Modeling the geochemical evolution of mine waters during mixing. J. Hazard Mater., 134929 https://doi.org/10.1016/j.jhazmat.2024.134929.

Sánchez-España, J., Pamo, E.L., Santofimia, E., Aduvire, O., Reyes, J., Barettino, D., 2005. Acid mine drainage in the Iberian Pyrite Belt (Odiel river watershed, Huelva, SW Spain): geochemistry, mineralogy and environmental implications. Appl. Geochem. 20 (7), 1320–1356. https://doi.org/10.1016/j.apgeochem.2005.01.011.

Sánchez-España, J., Pamo, E.L., Pastor, E.S., 2007. The oxidation of ferrous iron in acidic mine effluents from the Iberian Pyrite Belt (Odiel Basin, Huelva, Spain): field and laboratory rates. J. Geochem. Explor. 92 (2–3), 120–132. https://doi.org/10.1016/j.gexplo.2006.08.010.

Sánchez-España, J., Yusta, I., Diez-Ercilla, M., 2011. Schwertmannite and hydrobasaluminite: a re-evaluation of their solubility and control on the iron and aluminium concentration in acidic pit lakes. Appl. Geochem. 26 (9–10), 1752–1774. https://doi.org/10.1016/j.apgeochem.2011.06.020.

Santos, E.S., Abreu, M.M., Macías, F., 2019. Rehabilitation of mining areas through integrated biotechnological approach: technosols derived from organic/inorganic wastes and autochthonous plant development. Chemosphere 224, 765–775. https://doi.org/10.1016/j.chemosphere.2019.02.172.

Sarmiento, A.M., Nieto, J.M., Olías, M., Cánovas, C.R., 2009. Hydrochemical characteristics and seasonal influence on the pollution by acid mine drainage in the Odiel river Basin (SW Spain). Appl. Geochem. 24 (4), 697–714. https://doi.org/10.1016/j.apgeochem.2008.12.025.

Schemel, L.E., Cox, M.H., Runkel, R.L., Kimball, B.A., 2006. Multiple injected and natural conservative tracers quantify mixing in a stream confluence affected by acid mine drainage near Silverton, Colorado. Hydrol. Process.: Int. J. 20 (13), 2727–2743. https://doi.org/10.1002/hyp.6081.

Schoepfer, V.A., Burton, E.D., 2021. Schwertmannite: a review of its occurrence, formation, structure, stability and interactions with oxyanions. Earth Sci. Rev. 221, 103811. https://doi.org/10.1016/j.earscirev.2021.103811.

Swanson, D.A., Barbour, S.L., Wilson, G.W., 1997. Dry-site versus wet-site cover design. Proceedings of the Fourth International Conference on Acid Rock Drainage 4, 1595–1610.

Tamura, H., Goto, K., Yotsuyanagi, T., Nagayama, M., 1974. Spectrophotometric determination of iron (II) with 1, 10-phenanthroline in the presence of large amounts of iron (III). Talanta 21 (4), 314–318. https://doi.org/10.1016/0039-9140(74)80012-3.

Tu, Z., Wu, Q., He, H., Zhou, S., Liu, J., He, H., et al., 2022. Reduction of acid mine drainage by passivation of pyrite surfaces: a review. Sci. Total Environ. 832, 155116. https://doi.org/10.1016/j.scitotenv.2022.155116.

Vicente-Serrano, S.M., Tomas-Burguera, M., Beguería, S., Reig, F., Latorre, B., Peña-Gallardo, M., Luna, Y., Morata, A., González-Hidalgo, J.C., 2017. A high resolution dataset of drought indices for Spain. Data 2 (3), 22. https://doi.org/10.3390/data2030022.

Walton-Day, K., Mast, M.A., Runkel, R.L., 2021. Water-quality change following remediation using structural bulkheads in abandoned draining mines, upper Arkansas River and upper Animas River, Colorado USA. Appl. Geochem. 127, 104872. https://doi.org/10.1016/j.apgeochem.2021.104872.

Webster, J.G., Swedlund, P.J., Webster, K.S., 1998. Trace metal adsorption onto an acid mine drainage iron (III) oxy hydroxy sulfate. Environmental Science & Technology 32 (10), 1361–1368. https://doi.org/10.1021/es9704390.

World Health Organization, 2022. Guidelines for Drinking-Water Quality: Fourth Edition Incorporating the First and Second Addenda. World Health Organization (WHO), Geneva, 978-92-4-004506-4. https://www.who.int/publications/i/item/9789240045064.

Yesares, L., González-Jiménez, J.M., Jiménez-Cantizano, F.A., González-Pérez, I., Caro-Moreno, D., Sánchez, I.M., 2023. Unveiling high-tech metals in roasted pyrite wastes from the Iberian Pyrite Belt, SW Spain. Sustainability 15 (15), 12081.

Yu, J.Y., Heo, B., Choi, I.K., Cho, J.P., Chang, H.W., 1999. Apparent solubilities of schwertmannite and ferrihydrite in natural stream waters polluted by mine drainage. Geochem. Cosmochim. Acta 63 (19–20), 3407–3416. https://doi.org/10.1016/S0016-7037(99)00261-6.